

The historical fingerprint and future impact of climate change on childhood malaria in Africa

Colin J. Carlson^{1,*†}, Tamma A. Carleton^{2,*}, Romaric C. Odoulami³ and Christopher H. Trisos³

¹*Center for Global Health Science & Security, Georgetown University*

²*Bren School of Environmental Science & Management, University of California Santa Barbara*

³*African Climate and Development Initiative, University of Cape Town*

**These authors share lead author status.*

†Correspondence should be directed to colin.carlson@georgetown.edu.

Submitted to *medRxiv* on July 25, 2023

Abstract

The health burden of anthropogenic climate change is growing exponentially, but present-day impacts remain difficult to measure^{1,2,3}. Here, we leverage a recently-published comprehensive dataset of 50,425 population surveys⁴ to investigate whether human-caused climate change has increased the burden of childhood malaria across sub-Saharan Africa. In historical data, we find that prevalence shows a robust response to temperature and extreme precipitation, consistent with expectations from previous empirical and epidemiological work. Comparing historical climate reconstructions to counterfactual simulations without anthropogenic warming, we find two-to-one odds that human-caused climate change has increased the overall prevalence of childhood malaria across sub-Saharan Africa since 1901. We estimate that by 2014, human-caused climate change was responsible for an average of 84 excess cases of malaria per 100,000 children ages 2 to 10, with higher elevation and cooler regions in southern and east Africa having greater increases. Under future climate change, we project increasing temperatures could plausibly accelerate the eradication of malaria in west and central Africa, where the present-day burden is highest, leading to continent-wide average reductions of 89 (low greenhouse gas emissions, SSP1-RCP2.6) to 1,750 (high emissions, SSP5-RCP8.5) cases per 100,000 children by the end of the century. However, we find that limiting future global warming to below 2°C (SSP1-RCP2.6) compared to ~3°C (SSP2-RCP4.5) could prevent an average of 496 excess cases in southern Africa, and 40 excess cases in east Africa, per 100,000 children by 2100. Our study resolves a decades-old debate about one of the earliest health impacts of global warming, and provides a template for future work measuring the true global burden of climate change.

35 Main Text

36 Despite progress towards global eradication, malaria remains the single deadliest climate-
37 sensitive infectious disease⁵. Malaria transmission is highly responsive to temperature,
38 driven by both the life cycle of the ectothermic mosquito vectors (*Anopheles* spp.) and
39 the thermal sensitivity of the parasites (*Plasmodium* spp.) themselves^{6,7}. In laboratory
40 conditions, *P. falciparum* transmission by *An. gambiae* peaks around 25°C, and becomes
41 negligible below ~16°C or above ~34°C^{6,7,8}. Given these biological constraints, climate
42 change has become a major concern for populations in southern and high-elevation east
43 Africa, where colder temperatures once limited transmission^{9,10,11}. On the other hand, in
44 west and central Africa—where the burden of malaria is highest—many studies suggest
45 that climate change will reduce or eventually preclude transmission^{9,10,12,13}.

46 These risks were among the first proposed health impacts of climate change^{14,15},
47 but have been surprisingly contentious, and even described as “hot air”¹⁶ and “danger-
48 ous pseudoscience”¹⁷. Malaria experts have often claimed that observed warming trends
49 trends are incompatible with long-term reductions in prevalence across the continent, and
50 warned that other factors like drug resistance and funding instability pose a more serious
51 threat to malaria eradication^{16,18,19}. Empirical evidence to test these assumptions is
52 sparse, with the highest profile studies focusing on a single dataset of malaria incidence
53 over several decades at a tea plantation in Kericho, Kenya. Since 2000, over a dozen stud-
54 ies have argued that these data either support^{20,21,22,23,24} or undermine^{25,26,27,28,29,30,31}
55 the broader hypothesis that climate change is responsible for a resurgence of malaria in
56 the east African highlands^{28,32,33,34,35}. More recently, a study by Snow *et al.*⁴ examined
57 the last century of continent-wide changes in malaria prevalence, and concluded that
58 observed trends could not be neatly explained by climate change, but did so based only
59 on visual correspondence between moving averages of rainfall, minimum temperature,
60 and modeled malaria prevalence over the entire continent.

61 In this study, we revisit these debates by applying frontier methods from detection and
62 attribution, an area of climate science that quantifies the historical and real-time climate
63 impacts of anthropogenic greenhouse gas emissions^{36,37}. These methods underpin the
64 scientific consensus on human-caused climate change, and are regularly used to identify
65 the role of climate change in the intensity, frequency, and distribution of specific extreme
66 events (e.g., heatwaves, heavy precipitation, and droughts)^{38,39,40}. However, attribu-
67 tion remains challenging for the downstream impacts of anthropogenic climate change
68 on people and ecosystems, and methodological frameworks for impact attribution are
69 still comparatively underdeveloped³⁶. Applications to infectious disease dynamics are
70 especially challenging, as relationships between climate and disease transmission are of-
71 ten complex, nonlinear, and confounded by human intervention, and few epidemiological
72 datasets exist with sufficient spatial and temporal scope to resolve these relationships. As
73 a result, hundreds of studies have tested for correlations between climate and observed
74 changes in disease incidence or prevalence, but very few have shown that these changes
75 are causally attributable to anthropogenic climate change^{41,1}.

76 Here, we draw on frameworks from climate science^{38,39,40}, econometrics^{42,43}, and epi-
77 demiology^{41,1} to develop a single-step detection and attribution framework (per ref.⁴¹)

78 for the impacts of human-caused climate change on an infectious disease. We apply this
79 framework to estimates of *falciparum* malaria prevalence in children aged 2-10 in sub-
80 Saharan Africa ($PfPR_{2-10}$), which experiences roughly 95% of the global
81 burden of malaria (with 80% of deaths in children under the age of 5)⁴⁴. We analyze a
82 recently published dataset with unparalleled resolution and scope (Figure 1), consisting
83 of 50,425 surveys spanning more than a century (1900 to 2015)⁴, which we aggregate to
84 9,875 monthly average values at the first administrative (state or province) level. Lever-
85 aging climate econometric methods^{42,43,45,46}, we develop a panel regression model that
86 isolates the role of temperature and extreme precipitation from other confounding factors
87 that also shape malaria endemicity (Figure 2; see Methods for details). Nonparametric
88 controls in the model (called “fixed effects”) account for regional differences in seasonality,
89 time periods with concerted elimination efforts, and other spatiotemporal variation not
90 explained by identifiable factors, such as socioeconomic or ecological differences between
91 populations. To quantify statistical uncertainty in prevalence-climate relationships, we
92 repeatedly estimate the model with 1,000 spatially-blocked bootstrapped samples. We
93 apply these models to make predictions based on 10 sets of paired historical climate
94 simulations with and without anthropogenic climate forcing, and estimate the impact
95 of anthropogenic climate change on malaria prevalence from 1901 to 2014 (Figure 3).
96 Finally, we project how future climate change could further alter malaria prevalence
97 between 2015 and 2100, based on three future climate change scenarios for low (SSP1-
98 RCP2.6), intermediate (SSP2-RCP4.5), and high (SSP5-RCP8.5) future greenhouse gas
99 concentrations (Figure 4).

100 A robust signal of climate sensitivity

101 Over the last century, the prevalence of childhood malaria has exhibited a strong con-
102 cave relationship with temperature (Figure 2A). Closely tracking theoretical expectations
103 that *P. falciparum* transmission by *Anopheles gambiae* mosquitoes should peak around
104 25.6°C⁶, observed values of $PfPR_{2-10}$ in our dataset peak around a monthly mean tem-
105 perature of 25.8°C (Figure S1). Based on these biological expectations, we estimate the
106 effect of temperature as a quadratic response term in the panel regression model, and find
107 that prevalence peaks at 24.9°C (95% confidence interval across the 1,000 bootstrapped
108 models: 22.5°C, 27.0°C). These results confirm that laboratory-based studies approxi-
109 mate malaria epidemiology in real populations quite well, and that temperature plays a
110 substantial role in transmission dynamics: a 10°C increase or decrease from the optimal
111 temperature lowers prevalence by ~ 8 percentage points.

112 The relationship between precipitation and malaria prevalence is more complex, and
113 likely less consequential for historical trends (Figures 2B, 2C). Contemporaneous monthly
114 precipitation exhibits a nonlinear, but highly uncertain, relationship to prevalence (see
115 Figure S12). To parsimoniously capture nonlinear effects and disentangle divergent im-
116 pacts of low and high precipitation, we define precipitation shocks with two binary in-
117 dicator variables, equal to one when monthly precipitation falls below 10% (we label
118 this “drought”) or above 90% (we label this “flood”) percentiles of monthly precipitation
119 calculated for each subnational unit. While drought and flood events are complex phe-

120 nomena, which develop from the combination of multiple factors (e.g., soil conditions and
121 topography) in addition to rainfall over varying timescales, we use this terminology for
122 shorthand to indicate extremely low or high precipitation months. Although most effects
123 are statistically insignificant, we find that drought shocks tend to decrease malaria preva-
124 lence 1-2 months later, while conversely, flood shocks have a positive effect on prevalence
125 2-3 months later. These effects and their timing are broadly consistent with expectations
126 about how precipitation mediates the availability of mosquito breeding habitat: dry-out
127 kills larvae and eggs, while inundation creates new breeding habitat^{47,48,49,50,51,52,53,54}.
128 Sensitivity analyses were also weakly suggestive of another established mechanism, in
129 which floods may wash away eggs and larvae, reducing transmission in the shorter term
130 (see Figures S10 and S12). Overall, extreme precipitation has a measurable effect on
131 malaria prevalence, but may be less important than temperature; however, given the
132 sparsity of weather station data⁵⁵ and the uncertainty of precipitation reconstructions⁵⁶,
133 it is also possible that our analysis unavoidably underestimates the effect of these vari-
134 ables due to measurement error.

135 Additional sensitivity analyses reinforce that these prevalence-climate relationships
136 are both statistically robust and biologically consistent. Key findings are generally in-
137 sensitive to alternative model specifications, such as the inclusion of lagged effects of
138 temperature (Figure S7); higher-order polynomial effects of temperature (Figure S11);
139 alternative definitions of drought and flood shocks (Figures S8-S10); and alternative spa-
140 tiotemporal controls, which account differently for variation over space (at region, coun-
141 try, and state levels), time (including yearly and monthly variation), and interactions
142 among space and time (Figure S6 and Table S2).

143 **Historical impacts of climate change (1901-2014)**

144 We find that human-caused climate change has, more likely than not, been responsible for
145 a small increase in the average prevalence of childhood malaria across sub-Saharan Africa
146 since 1901 (Figures 2D). Compared to counterfactual simulations without anthropogenic
147 climate forcing, we estimate that by 2010-2014, climate change had caused an increase
148 in continental mean $PfPR_{2-10}$ of 0.08 percentage points (*p.p.*; 95% confidence interval:
149 -0.30 *p.p.*, 0.50 *p.p.*). Simulations with an attributable increase in continent-wide mean
150 prevalence outnumber those with losses by two to one (proportion P_+ of 10,000 paired
151 simulations with a positive difference = 0.66). These increases are almost entirely driven
152 by rising temperatures; the effects of drought and flood events on prevalence show no
153 distinguishable signal from anthropogenic emissions over time (Figure S4).

154 This overall trend masks substantial regional heterogeneity in historical climate change
155 impacts (Figure 3A; Figure S2), driven almost entirely by elevational and latitudinal gra-
156 dients in temperature (Figure 3B,C). For example, attributable impacts across southern
157 Africa are high in both magnitude and certainty, with an overall increase of 0.63 *p.p.*
158 (95% CI: -0.04 *p.p.*, 1.40 *p.p.*; $P_+ = 0.97$)—nearly an order of magnitude greater than
159 the continental mean. In contrast, climate change has contributed to significantly lower
160 malaria prevalence in west Africa (mean = -0.40 *p.p.*; 95% CI: -0.93 *p.p.*, 0.00 *p.p.*; $P_+ =$
161 0.03), where temperatures already often exceed the biological optimum for transmission.

162 In the central African basin, a stronghold of malaria endemicity with average tempera-
163 tures close to the 25°C optimum, the change in prevalence attributable to anthropogenic
164 climate change is positive, relatively small, and uncertain (mean = 0.18 *p.p.*; 95% CI:
165 -0.18 *p.p.*, 0.62 *p.p.*; $P_+ = 0.83$). Finally, we estimate a meaningful overall increase in
166 prevalence attributable to climate change in east Africa (mean = 0.34 *p.p.*; 95% CI: -0.13
167 *p.p.*, 0.87 *p.p.*; $P_+ = 0.91$), but note that impacts are distributed unevenly along the
168 steep elevational gradient: increases of up to 1-2 *p.p.* in the Ethiopian highlands and
169 the greater Rift Valley region are accompanied by small but significant local declines
170 throughout lowland areas in Ethiopia, Sudan, South Sudan, Eritrea, and Djibouti.

171 While these effects are meaningful, we caution that they are also far smaller than
172 the reduction achieved through healthcare, mosquito nets, vector control, and economic
173 development: previous work with the same dataset has estimated a reduction since 1900
174 of 16 *p.p.* (*i.e.*, a continent-wide decline in average $PfPR_{2-10}$ from 40% in 1900-1929
175 to 24% by 2010-2015⁴), while our estimates of historical climate-attributable changes
176 rarely exceed 2 *p.p.* for any individual administrative region. Additionally, we estimate
177 that average reductions in prevalence realized during the Global Malaria Eradication
178 Program (1955-1969; estimated reduction averaged over the entire period: -4.80 *p.p.*)
179 and recent programs like Roll Back Malaria and the Global Technical Strategy (2000–
180 2014; estimated reduction averaged over the entire period: -3.35 *p.p.*) were substantially
181 larger than the cumulative effects of anthropogenic climate change in most regions (Table
182 S2). Relatively small and spatially differentiated climate-related changes in burden could
183 have been easily concealed by the greater impact of these programs, highlighting both
184 the success of elimination programs and the importance of using an empirical approach
185 like ours that can isolate the effect of climate from other co-evolving factors.

186 **Future impacts of climate change (2015-2100)**

187 Despite contemporary trends, we project that within the next quarter-century, the net
188 impact of climate change will be a continent-wide reduction in malaria prevalence (Figure
189 2D; Table S1). This trend is driven largely by rising temperatures in lowland areas north
190 of the equator, with greater possible reductions in higher emissions scenarios (Figure 4).
191 In these scenarios, temperature-related declines are slightly offset by floods, which will
192 become more frequent across the continent³⁶, although their impact on overall trends
193 is trivial when compared to temperature (Figure S5). Even in a low emissions scenario
194 (SSP1-RCP2.6), present-day increases from historical warming would essentially be offset
195 by mid-century, stabilizing around an -0.08 *p.p.* (95% CI: -0.40 *p.p.*, 0.17 *p.p.*) projected
196 decline across sub-Saharan Africa (2048-2052, relative to 2015-2020). In a high emissions
197 scenario (SSP5-RCP8.5), we project that losses would accelerate over time, reaching an
198 average of -0.23 *p.p.* (95% CI: -0.79 *p.p.*, 0.26 *p.p.*) by mid-century and -1.8 *p.p.* (95%
199 CI: -4.6 *p.p.*, -0.03 *p.p.*) by the end of the century (2096-2100)—a reduction that would
200 be comparable in scale to some previous continent-wide eradication efforts.

201 Though the balance across regions will begin to shift, the geographic pattern of
202 future changes is likely to reproduce present-day heterogeneity in impacts, as malaria
203 transmission continues to shift along latitudinal and elevational clines in temperature

204 (Figure 4; Figure S3). West Africa will experience the most dramatic transformation,
205 especially in a high-emissions scenario (SSP5-RCP8.5), with a projected -1.0 *p.p.* (95%
206 CI: -1.9 *p.p.*, -0.35 *p.p.*) decline by mid-century, and a staggering -4.0 *p.p.* (95% CI:
207 -8.8 *p.p.*, -1.5 *p.p.*) region-wide decrease by 2100. Similar but shallower declines are
208 projected in central Africa, where end-of-century reductions could reach between -0.06
209 *p.p.* (SSP1-RCP2.6; 95% CI: -0.41 *p.p.*, 0.25 *p.p.*) and -1.2 *p.p.* (SSP5-RCP8.5; 95% CI:
210 -3.9 *p.p.*, 0.43 *p.p.*). On the other hand, localized increases will continue in the coldest
211 parts of the Ethiopian highlands, the greater Rift Valley region, and coastal southern
212 Africa, potentially reaching 5 percentage points or more in some areas. The overall effect
213 is positive across east and southern Africa, except in the highest emissions scenario: in
214 SSP5-RCP8.5, both regions start to experience declines by mid-century, with east Africa
215 eventually falling -0.48 *p.p.* (95% CI: -2.4 *p.p.*, 0.98 *p.p.*) below present-day levels.

216 Broadly, our results suggest that the main effect of climate change mitigation will
217 be to keep average temperatures in sub-Saharan Africa closer to the optimum range for
218 malaria transmission. However, for many colder localities, emissions reductions would
219 prevent substantial climate-driven increases in malaria prevalence. By mid-century,
220 compared to a medium emissions scenario similar to current global projections (SSP2-
221 RCP4.5)⁵⁷, keeping global warming below +2°C (the target simulated by SSP1-RCP2.6)
222 would prevent an estimated 163 excess cases of malaria per 100,000 children in southern
223 Africa, as well as 24 excess cases per 100,000 children in east Africa. By the end of the
224 century, these benefits would be even greater, with 496 and 40 excess cases averted per
225 100,000 children in southern and east Africa, respectively (Table S1). At a more local
226 scale, these benefits could be at least an order of magnitude greater (Figure S3).

227 Discussion

228 In this study, we apply a detection and attribution framework to a century of malaria
229 surveillance, allowing us to estimate the historical and projected future impact of an-
230 thropogenic climate change on childhood malaria in sub-Saharan Africa. Since 1901, we
231 find a 66% likelihood that anthropogenic climate change has increased malaria burden;
232 on average across the continent, an estimated 84 excess cases per 100,000 people can
233 be attributed to historical human-caused climate change. However, this burden falls
234 disproportionately on southern and east Africa; we estimate a 97% and 91% likelihood,
235 respectively, that anthropogenic climate change has increased present-day malaria preva-
236 lence in these regions, and project that prevalence in both will remain elevated through
237 2100, even in an emissions scenario likely to keep warming under the Paris Agreement
238 target of +2°C. However, across the continent, we project that the overall impact of
239 future climate change will be a net reduction in malaria: these changes will be most
240 dramatic in west and central Africa, where climate change could respectively prevent up
241 to ~4,000 and ~1,200 cases of malaria per 100,000 children in a high-emissions scenario.
242 In total, our results suggest that climate change could be synergistic with eradication
243 efforts in countries like Nigeria and the Democratic Republic of the Congo, where the
244 present-day burden of malaria is highest, but will continue to create new risks in countries
245 like Ethiopia and South Africa.

246 Spanning two centuries, our analysis is the most comprehensive look to date at the
247 impact of climate change on any infectious disease, and brings new clarity to a decades-
248 long debate in malaria research. Whereas some work has questioned the plausibility that
249 overall declines in continent-wide prevalence would conceal a climate-linked increase^{4,19},
250 the 0.08 percentage point increase in $PfPR_{2-10}$ that we attribute to historical climate
251 change could easily be masked by the 200-fold greater reduction observed across sub-
252 Saharan Africa over the same period. Our regional estimates also generally align with
253 previous lab-based or site-specific empirical work, which suggests that east and southern
254 Africa are experiencing shifts towards temperatures that are permissive to transmission
255 for the first time or over longer seasons^{9,10}, while in west and central Africa, climate
256 change impacts have been harder to detect, and future warming might exceed the physi-
257 ological limits of malaria transmission^{9,10,13,58}. Notably, our study does provides robust,
258 empirical evidence that climate change has at least marginally contributed to malaria
259 resurgence in high-altitude Kenya and Ethiopia, consistent with local epidemic time series
260 or simulated dynamics based on local weather station data^{21,24,34}.

261 Our study reconciles three long-standing ideas that are sometimes treated as para-
262 doxical: climate change is not the primary force shaping past, or probably future, trends
263 in malaria prevalence^{4,16,19}; however, climate change has increased the burden of malaria
264 in sub-Saharan Africa^{14,15,21,24}, and at high elevations and latitudes, will continue to for
265 several decades^{9,10}; nevertheless, rising temperatures will mostly assist future efforts to
266 eradicate *Plasmodium falciparum* from sub-Saharan Africa^{10,19,58}. In spite of climate
267 change, elimination campaigns have already achieved substantial reductions in malaria
268 endemicity over the last century. This history underscores the value of disease surveil-
269 lance, healthcare, and vector control as core components of climate change adaptation,
270 as well as the plausibility of malaria eradication within a generation⁵⁹—a point echoed
271 by the recent work on the elimination of malaria from Hainan Island in China⁶⁰. At the
272 same time, several recent anecdotes have raised relevant concerns about the fragility of
273 elimination, such as the resurgence of malaria in Ecuador and Peru driven by mass migra-
274 tion from Venezuela⁶¹, or the estimated 10,000 excess deaths and 3.5 million untreated
275 malaria cases caused by healthcare disruptions during the 2014 Ebola virus epidemic in
276 West Africa⁶². Concerns about climate-linked resurgence are also more credible given the
277 ongoing invasion of the *An. stephensi* mosquito, which thrives in cities, has already been
278 reported in several locations in east Africa, and may be able to transmit *P. falciparum*
279 up to much higher temperatures ($\sim 37^{\circ}\text{C}$) than *An. gambiae* can ($\sim 30^{\circ}\text{C}$)^{8,63}. If *An.*
280 *stephensi* were to become a dominant vector across the continent, climate change might
281 become an even more pressing concern^{64,65}. These risks only add more urgency to the
282 global goals of eliminating both malaria and greenhouse gas emissions.

283 Methods

284 Malaria prevalence data

285 We use a recently published database of *Plasmodium falciparum* clinical prevalence in
286 Sub-Saharan Africa⁴. This compendium, compiled by Snow *et al.* over more than
287 two decades, is one of the most spatially and temporally complete publicly-available
288 databases of infectious disease burden. The database covers the period from 1900 to
289 2015, though sampling has increased substantially since the turn of the century (pre-2000:
290 $n = 32,533$; post-2000: $n = 17,892$). Most prevalence surveys used microscopy for diag-
291 nostics ($n = 36,805$) but a substantial portion of data also derive from rapid diagnostic
292 tests ($n = 11,154$). The data have been compiled from a mix of archival research through
293 public health documents, including the records of colonial governments and elimination
294 campaigns from different periods; national survey data; electronic records published in
295 peer-reviewed journals and grey data sources (e.g., World Health Organization technical
296 documents); and a mix of other sources compiled by international organizations. Records
297 were georeferenced in the original study using a standard set of protocols, with a 5km
298 grid uncertainty threshold for point data, and broader areas stored as administrative
299 polygons. In total, the data include a total of 50,425 prevalence surveys at a total of
300 36,966 unique georeferenced locations.

301 For our models, we used the estimates of malaria prevalence for children aged two
302 to ten years old, as *falciparum* malaria has the highest mortality in children and preg-
303 nant women. The Snow *et al.* data cover all available prevalence surveys, including all
304 age ranges, but were converted by the authors of the original study to a standardized
305 estimate of prevalence in children aged 2-10 ($PfPR_{2-10}$), using a catalytic conversion
306 Muench model. For our model, we aggregated data by averaging $PfPR_{2-10}$ at the first
307 administrative level within-country (i.e., state or province level, or as shorthand, ADM1),
308 using shapefiles provided by the Database of Global Administrative Areas dataset version
309 3.6 (www.gadm.org). This provided sufficient granularity to capture climate impacts and
310 local heterogeneity in confounders, while ensuring sufficient data coverage within these
311 units. This aggregation scale is supported by previous work that models this dataset at
312 the same spatial resolution⁴.

313 Climate data

314 We used two sets of climate data in this study. The first is an observational dataset from
315 the Climatic Research Unit (hereafter, CRU-TS; version 4.03 for model training and
316 4.06 for bias correction), which is constructed from monthly observations from extensive
317 networks of meteorological stations from around the globe⁶⁶. CRU-TS provides land-
318 only climatic variables at a high spatial resolution of $0.5^\circ \times 0.5^\circ$ extending from 1901 to
319 present (though our analysis is limited to the period 1901-2014). The second set of data
320 is from ten global climate models (GCMs) selected from the sixth phase of the Coupled
321 Model Intercomparison Project (CMIP6). In our historical analysis, we analysed (per
322 GCM) one model realization of the “Historical” simulation, which includes anthropogenic

323 greenhouse gas emissions, and one realization from the “Historical-Natural” simulation,
324 which includes only solar and volcanic climate forcing. For both the Historical and
325 Historical-Natural (hereafter and in the main text, “historical climate” and “historical
326 counterfactual”) simulations, we analysed the period 1901-2014.

327 To investigate the continued effect of climate change on malaria prevalence between
328 2015 and 2100, we analysed three CMIP6 future climate change simulations from each
329 of the 10 GCMs. Shared socio-economic pathways (SSPs) refer to the level of potential
330 future global development (social, economic, and technological) and the implication for
331 climate change mitigation and/or adaptation actions or policy^{67,68}. SSPs are combined
332 with various possible future radiative forcings (representative concentration pathways;
333 RCPs) to form the climate change scenarios used in CMIP6. Of the available SSP–RCP
334 scenarios, we selected and used three. The first two suggest enhanced human develop-
335 ment outcomes with increased potential towards a more sustainable (SSP1⁶⁹) or a less
336 sustainable (SSP5⁷⁰) economy. The third, SSP2⁷¹, is a mid-way scenario, which assumes
337 a future that mostly follows historical trends⁶⁸. We selected these scenarios in combina-
338 tion with a low (SSP1-RCP2.6), intermediate (SSP2-RCP4.5), and high (SSP5-RCP8.5)
339 greenhouse gas concentration scenario.

340 We apply a standard quantile-quantile (Q-Q) bias-correction^{72,73} to the CMIP6 pre-
341 cipitation and temperature datasets for both of the historical simulations for the period
342 1901-2014, and all three future simulations for the period 2015-2100. Before the bias-
343 correction, we first remap all simulated CMIP6 precipitation and temperature datasets
344 to the same grid cell size ($0.5^\circ \times 0.5^\circ$) as the CRU-TS observation data. We then per-
345 form for each CMIP6 model, the Q-Q bias correction at each grid-point by mapping the
346 quantile values (q_i) for the empirical cumulative distribution functions for each of the 12
347 months over the period 1901-2014 (for each grid point) onto the corresponding quantiles
348 in the observational dataset (CRU-TS), so that the observed precipitation or tempera-
349 ture values associated with q_i become the bias-corrected value in the simulations. For
350 the counterfactual (and future) simulations, we first determine, at each grid-point, for
351 each value of precipitation or temperature (for each month) over the period 1901-2014
352 (2015-2100) the equivalent quantile (q_j) in the factual simulation and then identify the
353 precipitation or temperature value associated with q_j in the observational dataset as the
354 bias-corrected value. We detrended both precipitation and temperature datasets before
355 applying the bias-correction procedure, and then added the trends back after⁷³.

356 For every climate dataset (all CRU-TS and CMIP6 models), we extract the average
357 value of monthly precipitation and temperature within each ADM1 unit. To construct
358 polynomial variables for temperature and precipitation (see below), all data were trans-
359 formed at the grid cell level prior to aggregation to the ADM1 unit; extreme precipitation
360 cutoffs were defined at the ADM1 level and so were applied after aggregation.

361 Statistical model

362 The influence of climatic conditions on malaria prevalence has been heavily studied us-
363 ing transmission models based in vector ecophysiology and calibrated using laboratory
364 experiments^{6,7}. The important benefit of this approach is that the mechanistic links

365 between a particular environmental condition (e.g., temperature) and malaria prevalence
366 in the human population, such as effects on biting rate and survival probability, can be
367 independently isolated. However, this approach is limited in its ability to generalize to
368 real-world contexts, where complex socioeconomic factors interact with modeled relation-
369 ships based on laboratory conditions. Clinical data, which measures malaria prevalence
370 in human populations, has been used to validate modeled results (e.g., ref.⁶), but incon-
371 sistent findings arise due to challenges in statistically isolating the role of climate from the
372 many correlated factors influencing prevalence, such as public health interventions, drug
373 resistance, conflict and social instability, and economic shocks (e.g., refs.^{74,19,75,58,76}).

374 This study seeks to provide generalizable population-scale evidence of the malaria-
375 climate link across sub-Saharan Africa using field-collected clinical data and a statistical
376 approach designed to isolate changing environmental conditions from spatiotemporal con-
377 founding factors. Specifically, we draw on the climate econometrics literature⁷⁷, which
378 has developed causal inference approaches to quantify and project the impacts of anthro-
379 pogenic climate change on a host of socioeconomic outcomes, from agricultural yields⁷⁸,
380 to civil conflict⁷⁹, to all-cause mortality⁴⁶. This approach is designed to approximate
381 controlled experiments by semi-parametrically accounting for unobservable spatial and
382 temporal confounding factors, isolating variation in the climate system that is as good as
383 randomly assigned⁸⁰. This approach is often referred to as “reduced-form”, as it allows for
384 a causal interpretation of recovered relationships between socioeconomic conditions and
385 the climate, but it does not easily enable the researcher to isolate individual *mechanisms*
386 linking a changing climate to shifts in outcomes (e.g., mosquito population dynamics or
387 parasite development rates). However, causal estimates enable counterfactual simulation
388 in which climate is changed and all other factors are held constant; this is the exercise
389 conducted here and in many applications of climate econometric frameworks. More-
390 over, these relationships can be used to calibrate more structured transmission models
391 by providing empirical grounding from observational data.

392 We develop a statistical model using monthly survey-based malaria prevalence data
393 for children aged 2-10 ($PfPR_{2-10}$) covering all of sub-Saharan Africa over 115 years.
394 Our outcome variable is the average prevalence for each first administrative unit i (e.g.,
395 province or state) in country c during month m and year t , which we denote $PfPR_{icmt}$.
396 We estimate prevalence as a flexible function of monthly temperature T_{icmt} and precipi-
397 tation P_{icmt} variables as follows:

$$PfPR_{icmt} = f(T_{icmt}) + \sum_{\ell=0}^L g_{\ell}(P_{icm-\ell t}) + \alpha_i + \gamma_{rm} + h_c(\text{date}_{mt}) \quad (1)$$
$$+ \delta_1 \mathbb{1}\{\text{intervention 1}\}_{mt} + \delta_2 \mathbb{1}\{\text{intervention 2}\}_{mt} + \varepsilon_{icmt}$$

398 where $f(\cdot)$ and $g(\cdot)$ represent nonlinear transformations of grid-cell level temperature and
399 precipitation conditions, respectively, and where ℓ subscripts indicate monthly temporal
400 lags. In our main specification, we model $f(\cdot)$ as a quadratic in contemporaneous average
401 temperature, while $g(\cdot)$ contains a vector of dummy variables indicating whether an

402 administrative unit’s monthly rainfall can be categorized as drought (defined as $\leq 10\%$
403 of the long-run location- and month-specific mean) or flood (defined as $\geq 90\%$ of the
404 long-run location- and month-specific mean) during month $m - \ell$. We allow for up to
405 three monthly lags (i.e., $L = 3$) for these extreme precipitation conditions in our
406 main specification, based on hypotheses from prior literature regarding the timescales of
407 larvae drying and of “flushing”^{47,50,81}. A variety of sensitivity analyses detailed below
408 demonstrate that key findings are robust to including lags for temperature (Figure S7), to
409 the drought and flood cutoffs used for precipitation (Figures S8-S10), and to alternative
410 functional forms of temperature (Figure S11).

411 Equation 1 uses a suite of semi-parametric spatiotemporal controls to isolate plau-
412 sibly random variation in climatological conditions, following standard practices in the
413 climate impacts literature.^{77,43} First, α_i is a vector of indicator variables for each of 853
414 first administrative units (i.e., “ADM1” units) across our multi-country sample. These
415 spatial “fixed effects” control for all time-invariant characteristics of an administrative
416 unit that may confound the relationship between temperature, rainfall, and prevalence.
417 For example, higher altitude regions may exhibit cooler temperatures, but they also may
418 be composed of lower-income and more geographically isolated communities with lim-
419 ited access to malaria prevention interventions. By controlling for mean conditions in
420 each location, these spatial fixed effects avoid conflating climate conditions with other
421 geographic correlates.

422 Second, γ_{rm} is a vector of region-by-month-of-year indicator variables, where regions
423 are defined using the Global Burden of Disease (GBD) regional definitions of Western,
424 Southern, Central, and Eastern Africa (see Figure 2 in ref.⁸²). These spatiotemporal
425 fixed effects account for region-specific seasonality in prevalence that may spuriously
426 relate to seasonally-varying climatological conditions. We allow these seasonal controls
427 to vary by region because of large differences in climatological seasonality and in malaria
428 cyclicity across sub-Saharan Africa⁸³, and we show below that our main findings are
429 robust to more stringent seasonality controls defined at the country level (Figure S6).
430 Third, $h_c(\cdot)$ is a nonlinear, country-specific function that controls for country-specific
431 gradual trends that may confound the malaria-climate relationship, particularly under
432 historical conditions of anthropogenic climate change. In our main specification, we
433 model $h_c(\cdot)$ as a quadratic. Figure S6 shows that our results are robust to multiple
434 alternative approaches to controlling for long-run trends that may vary across space.

435 Finally, the indicator variables $\mathbb{1}\{\text{intervention 1}\}_{mt}$ and $\mathbb{1}\{\text{intervention 2}\}_{mt}$ are equal
436 to one when an observation falls into the 1955-1969 or 2000-2015 period, respectively.
437 These two periods saw substantial malaria intervention programs across the subconti-
438 nent, leading to considerable declines in malaria that were unrelated to changes in the
439 climate^{4,84}. These indicator variables control for shocks to prevalence during these two
440 periods, and the coefficients δ_1 and δ_2 allow for differential effectiveness of the two dis-
441 tinct intervention periods. While these variables are highly statistically significant (Table
442 S2), our main findings are robust to their exclusion (Figure S6).

443 Together, these set of flexible controls imply that the residual variation in temperature
444 and precipitation events used to identify the functions $f(\cdot)$ and $g(\cdot)$ is month-to-month

445 variation over time within the same location, after controlling for gradual country-specific
446 trends, regional seasonality, and the aggregate effects of two substantial malaria preven-
447 tion intervention programs. When reporting regression results directly, we cluster stan-
448 dard errors ε_{icmt} at the ADM1 level to account for serial correlation within the same
449 location. When computing bootstrap samples (e.g., shown in Figure 2), we repeatedly
450 re-estimate Equation 1 after block-resampling the full dataset using ADM1-level blocks
451 to account for this same serial correlation.

452 **Statistical model sensitivity and robustness**

453 In this section, we describe a set of model sensitivity analyses that probe the robustness
454 of our empirical model. Specifically, we investigate sensitivity of our key findings to:
455 alternative spatiotemporal controls; inclusion of dynamic temperature effects; alternative
456 definitions of extreme rainfall events; and alternative functional forms for the prevalence-
457 temperature relationship.

458 **Alternative spatiotemporal controls**

459 Our preferred empirical specification in Equation 1 includes first administrative unit fixed
460 effects (i.e., indicator variables), region-by-month-of-year fixed effects, country-specific
461 quadratic time trends, and two indicator variables for each of two malaria intervention
462 periods (1955-1969 and 2000-2015). Figure S6 shows that our estimated prevalence-
463 temperature relationship is highly robust to many alternative spatial and temporal con-
464 trols. All panels in this figure include ADM1 fixed effects to control for time-invariant
465 characteristics that may confound the relationship between prevalence and temperature,
466 but each panel varies in the additional spatial and/or temporal controls included in the
467 regression. A tabular version of these results is shown in Table S2. While the temper-
468 ature at which prevalence peaks changes slightly across model specifications, it remains
469 within a degree of the 25°C value from our preferred specification for most models,
470 particularly those including time trends that are spatially differentiated. Predictably,
471 stringent controls, such as region-by-year and country-by-month fixed effects, tend to in-
472 crease statistical uncertainty. However, overall the estimated shape and magnitude of the
473 prevalence-temperature relationship remain robust to alternative spatial and temporal
474 controls.

475 **Dynamic temperature effects**

476 Our preferred empirical specification estimates contemporaneous (within one month) and
477 lagged (up to three months) effects of extreme rainfall on malaria prevalence, but only
478 contemporaneous effects of temperature. While it is possible that temperature also ex-
479 hibits lagged effects, we show in Figure S7 that the cumulative effect of temperature on
480 $PfPR_{2-10}$ is very similar whether zero, one, two, or three months of lagged temperatures
481 are accounted for. The prevalence response to temperature does become slightly stronger
482 with three months of lags, suggesting that our historical and future climate projections

483 shown throughout the main text may be somewhat conservative. However, overall these
484 findings suggest that climate change impact projections are unlikely to change meaning-
485 fully under different assumptions of the lag structure of temperature exposure.

486 **Alternative definitions of extreme rainfall events**

487 Our main empirical specification defines drought as months for which total precipitation
488 is less than or equal to 10% of the long-run location- and month-specific mean. Flood is
489 analogously defined as months for which total precipitation is greater than or equal to 90%
490 of the long-run location- and month-specific mean. Here, we investigate the sensitivity
491 of our main findings to these definitions. To do so, we systematically vary both the
492 drought and flood cutoff values, ranging from <1% to <20% for drought and from >85%
493 to >95% for flood. Figure S8 shows that the relationship between malaria prevalence and
494 temperature is insensitive to the definition of drought and flood events. Figure S9 shows
495 that under most drought and flood definitions, extremely low precipitation events have
496 a negative effect on prevalence with a lag of 1-2 months. However, this effect is rarely
497 statistically significant. Figure S10 shows that extremely high rainfall events increase
498 prevalence with a lag of 2-3 months, a result is statistically significant and highly robust
499 to alternative drought and flood definitions. In general, these sensitivity analyses show
500 that our main findings are not sensitive to the specific definitions of drought and flood
501 used in estimation of Equation 1.

502 **Alternative functional forms for the prevalence-temperature relationship**

503 Following from theoretical and laboratory-based literature (e.g., refs.^{6,7}), we model the
504 prevalence-temperature relationship as quadratic. However, Figure S11 shows that this
505 relationship is similar when more flexible functional forms are used. In particular, the
506 temperature at which prevalence peaks changes little when higher order polynomials are
507 estimated. Estimating higher order polynomials increases uncertainty, particularly in the
508 tails of the temperature distribution, but point estimates are similar across the majority
509 of the temperature support.

510 **Projections**

511 In both historical and future simulations, we apply the panel regression to estimate
512 the effect of climate change on $PfPR_{2-10}$. Our predictions capture the full range of
513 statistical uncertainty (1,000 model estimates) and climate model uncertainty (10 climate
514 models), producing a total of 10,000 estimates of historical or future impacts in any given
515 scenario. Each of these 10,000 estimates is normalized to a long-run baseline (past: 1901-
516 1930; present: 2015-2020) before estimates are averaged, creating an estimate of climate
517 change impacts relative to that baseline. While the panel regression model accounts
518 for historical variation through the fixed effects structure, we do not examine overall
519 prevalence predictions for the historical model, and cannot apply it to predict future
520 overall prevalence (i.e., no future estimates exist for non-climate effects in the model).

521 For overall trends, we generated continent-wide averages or four regional averages
522 using the unweighted average of estimates for each ADM1 unit. This is a deliberate over-
523 simplification, as we do not adjust averages based on either ADM1 units' land area or
524 the estimated population they contain; we made this decision based on the challenges of
525 reconstructing historical population density at fine scales, as well as the need to otherwise
526 make assumptions about how disease burden is allocated over space (e.g., the distribution
527 of transmission across rural or urban areas). For similar reasons, we chose not to esti-
528 mate the effect of prevalence changes on overall malaria incidence. Although some studies
529 have attempted this using a linear conversion with total population⁸⁵, proper estimation
530 of incidence (and the effects of treatment variables, through prevalence, on case bur-
531 den) requires malaria transmission models that require substantially more demographic
532 assumptions⁸⁴. Future work could explore both of these methodologically-complex di-
533 rections, and potentially generate finer-scale estimates of how many cases of childhood
534 malaria, and resulting deaths, are attributable to climate change.

535 **Acknowledgements**

536 We thank Sadie Ryan and Rory Gibb for thoughtful conversations that supported this
537 work, and Jonathan Proctor for constructive feedback on the manuscript. CHT was
538 supported by the University of Cape Town Future Leaders Programme and by the FLAIR
539 Fellowship Programme: a partnership between the African Academy of Sciences and the
540 Royal Society funded by the UK Government's Global Challenges Research Fund. RCO
541 was supported by the Carnegie Corporation of New York through the Development of
542 Emerging Academic Leaders (DEAL) in Africa and the German Academic Exchange
543 Service (DAAD) ClimapAfrica programme.

544 **Data Availability**

545 No original data are generated or reported in our study. All data used in analyses,
546 including both malaria and climate data, is freely available and referenced in the Methods.

547 **Code Availability**

548 All code is available at github.com/cjcarlson/falciparum.

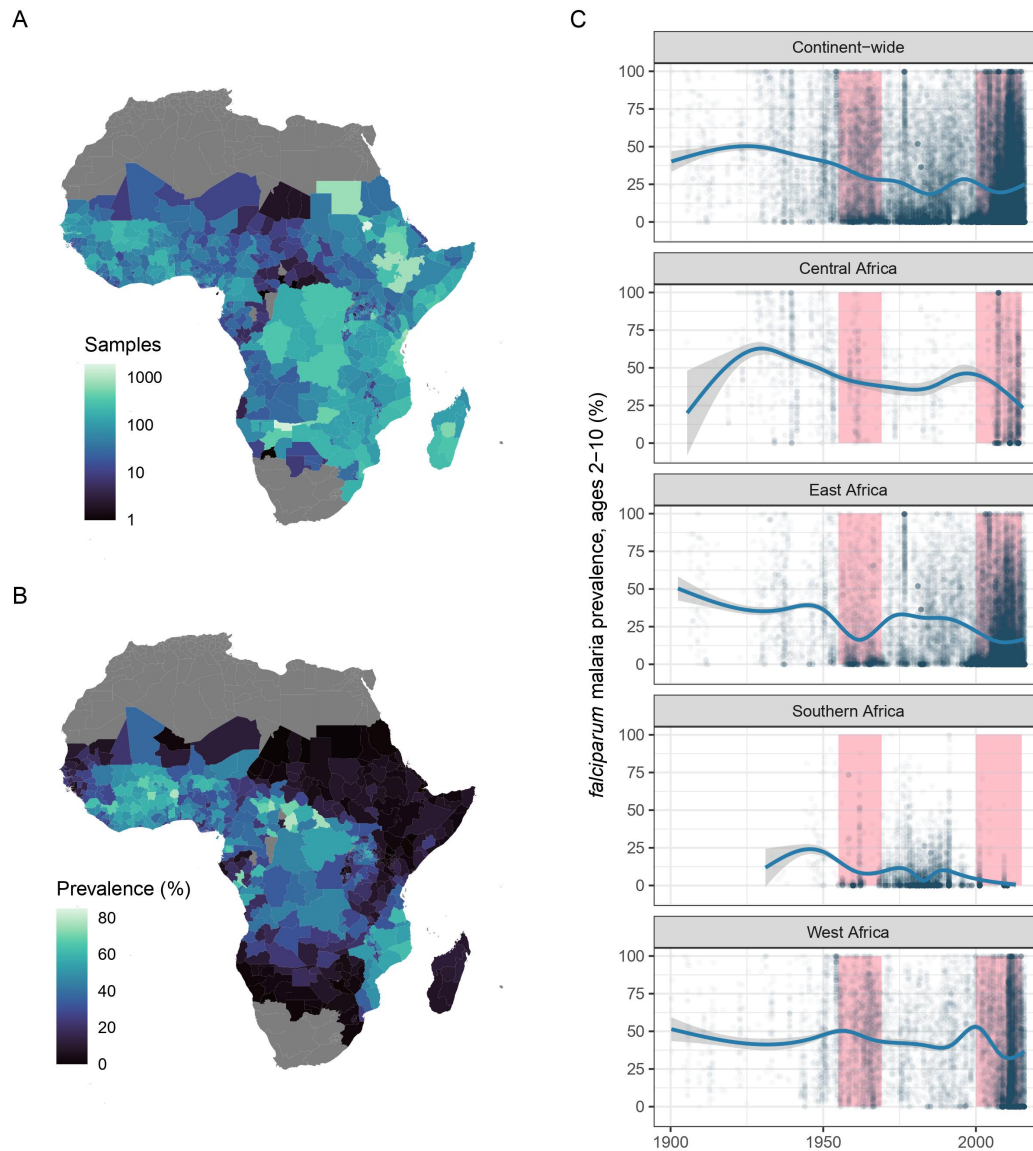


Figure 1: **Malaria prevalence observations from 1900 to 2015.** (A) The total number of malaria prevalence surveys in children ages 2 to 10 in the 20th and early 21st century, as measured by Snow *et al.*⁴ and aggregated to the first administrative unit (ADM1). (B) Mean reported prevalence of childhood malaria over the entire sample (1900-2015, with temporal coverage varying across space). (C) Observed trends in malaria prevalence, broken down by Global Burden of Disease Study regions (see main text): each point is a single survey in the original dataset, while generalized additive models are used to construct estimated trend lines (shown in solid blue, with grey shading showing the models' 95% confidence interval). Pink vertical bars indicate notable periods of successful malaria prevention intervention: the Global Malaria Eradication Programme (1955-1969) and the modern period including the Roll Back Malaria programs and Global Technical Strategy (2000-).

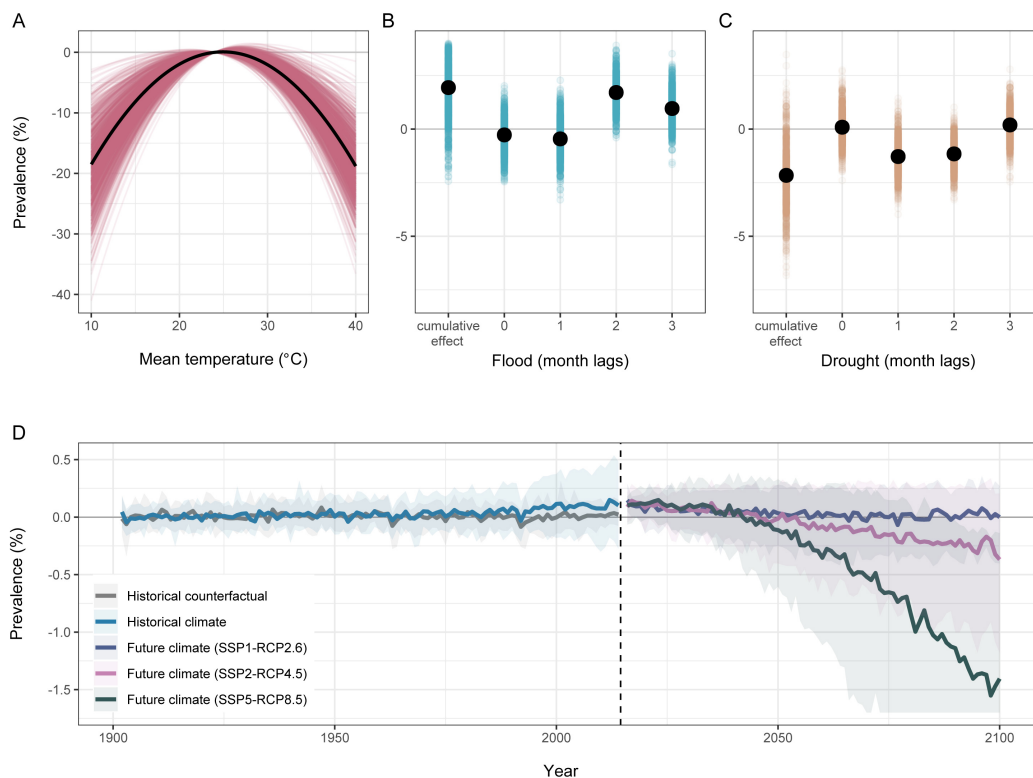


Figure 2: Empirical estimates of prevalence-climate relationships and predictions of climate change impacts from 1901 to 2100. (A) The estimated relationship between temperature and prevalence (point estimate in black line; bootstrapped estimates in red). (B,C) The effects of extreme precipitation events (flood and drought) in the month they occur (0 lag) and after time has passed (1, 2, 3 month lags), as well as the cumulative impact across the first three months; point estimates from the main model (black) are accompanied by bootstrap estimates (blue, brown). (D) Predicted change in prevalence attributable to climate change in the recent past (real historical climate given in blue; counterfactual without anthropogenic warming in grey) and in the future for three distinct climate pathways (blue: SSP1-RCP2.6; pink: SSP2-RCP4.5; green: SSP5-RCP8.5). Thick lines are the median estimates across all 10,000 simulations; shading indicates 5% and 95% percentiles of this distribution, and is truncated at the lower axis limits for visualization purposes (but the full interval is shown in Figure S5A). Historical estimates are shown relative to an average baseline across 1901 to 1930. Future estimates are shown relative to a baseline across 2015 to 2019, added to the end-of-historical baseline (2010 to 2014). Years with incomplete predictions due to lag effects (1901 and 2015) are not displayed.

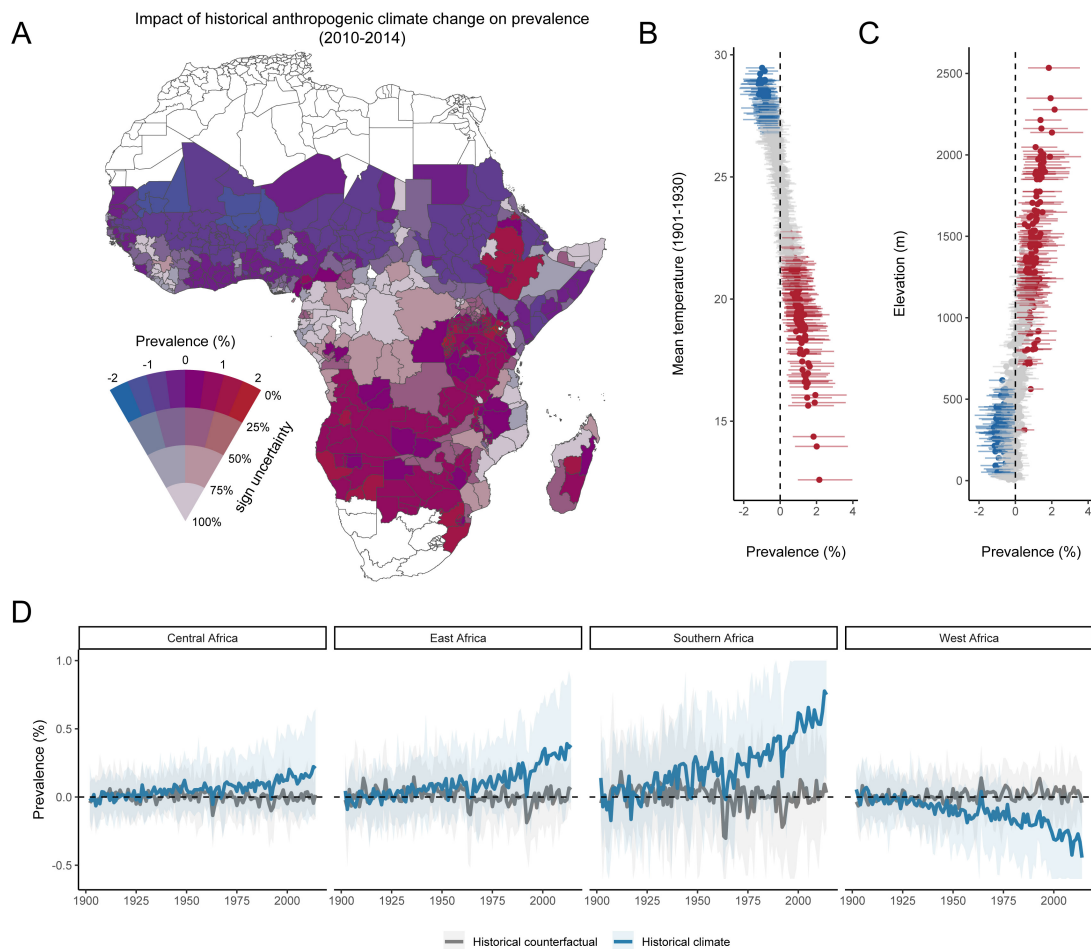


Figure 3: Historical changes in malaria prevalence attributable to climate change from 1901 to 2014. (A) Estimated climate-attributable change in prevalence in a polygon based on the difference between the historical climate in 2010-2014 and a counterfactual scenario for the same period simulated without anthropogenic warming. Sign uncertainty reports, across all 10,000 simulations, how many estimate the same direction of trend: an uncertainty of 0% implies that all models predict a positive or negative trend, while an uncertainty close to 100% indicates a near-even split. (B) Estimated climate-attributable change in prevalence in each administrative polygon, compared to the baseline mean temperature at the start of the 20th century; lines indicate 5% and 95% percentiles. (C) Estimated climate-attributable change in prevalence in each administrative polygon, compared to average elevation; lines indicate 5% and 95% percentiles. (D) Predicted changes by year, broken down by region. As in Figure 2, predictions based on true historical climate (blue) are compared to counterfactual predictions without anthropogenic warming (grey), relative to a 1901 to 1930 baseline. Thick lines are the median estimate across all 10,000 simulations; shading indicates 5% and 95% percentiles, and is truncated at the upper and lower axis limits for visualization purposes. Plots begin in 1902 with the first full year of predictions (due to lag effects).

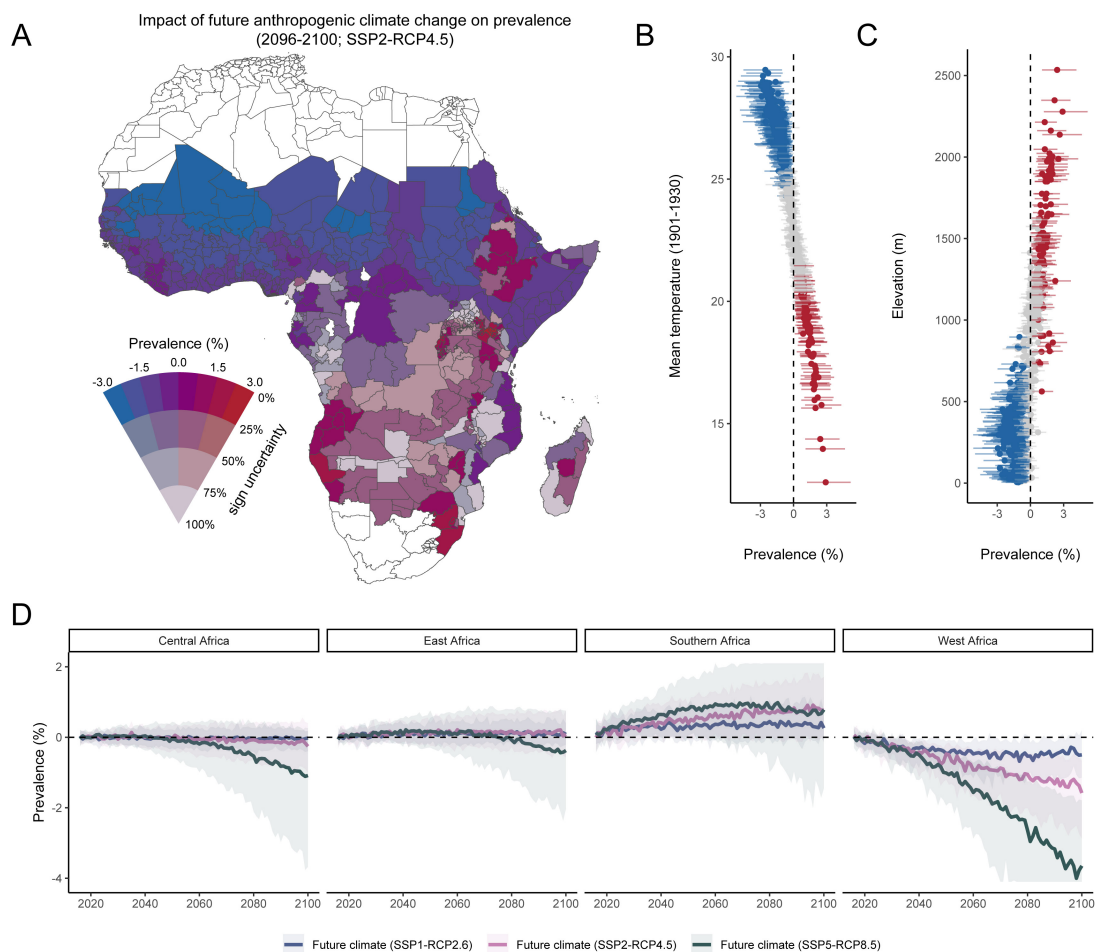


Figure 4: Projected future changes in malaria prevalence driven by climate change from 2015 to 2100. (A) Estimated climate-driven changes in prevalence by the end of the century (2096-2100), compared to the present day (2015-2020), in a medium emissions scenario (SSP2-RCP4.5). Sign uncertainty reports, across all 10,000 simulations, how many estimate the same direction of trend: an uncertainty of 0% implies that all models predict a positive or negative trend, while an uncertainty close to 100% indicates a near-even split. (B) Estimated climate-driven changes in prevalence in each administrative polygon, estimated for SSP2-RCP4.5, compared to the baseline mean temperature at the start of the 20th century; lines indicate 5% and 95% percentiles. (C) Estimated climate-driven changes in prevalence in each administrative polygon, estimated for SSP2-RCP4.5, compared to average elevation; lines indicate 5% and 95% percentiles. (D) Projected changes by year across all scenarios, broken down by region. Projections are given relative to the mean from 2015-2020, and as in Figure 2, and line color indicates scenario (blue: SSP1-RCP2.6; pink: SSP2-RCP4.5; green: SSP5-RCP8.5). Thick lines are the median estimate across all 10,000 simulations; shading indicates 5% and 95% percentiles, and is truncated at the upper and lower axis limits for visualization purposes. Plots begin in 2016 with the first full year of predictions (due to lag effects).

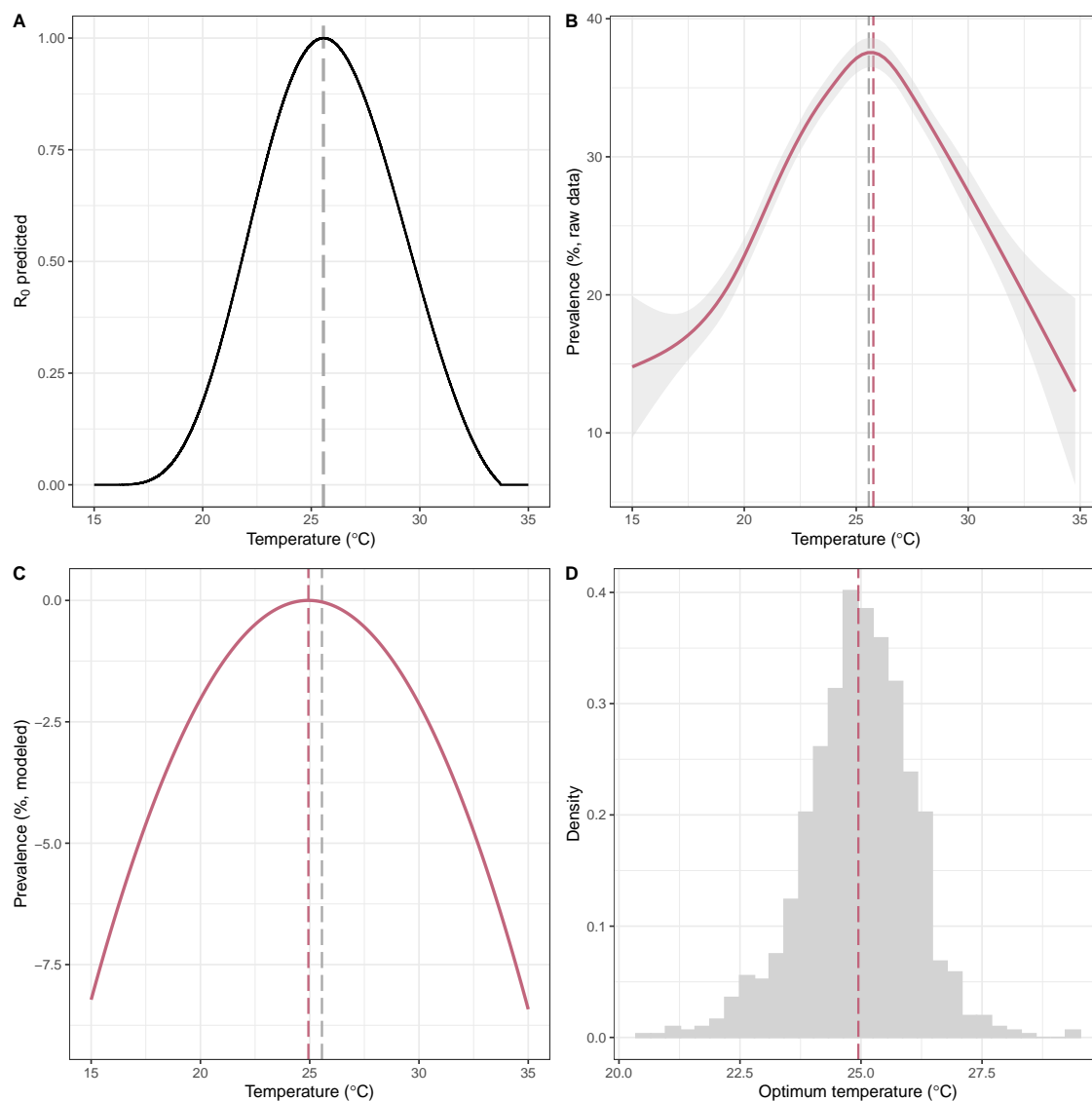


Figure S1: Malaria prevalence follows biological expectations. (A) The theoretical expectation for $R_0(T)$, the scaled partial response of the basic reproduction number to temperature, estimated based on empirical data (black line)⁶. Transmission peaks around an estimated optimum of 25.6 °C (grey dashed line). (B) Observed malaria prevalence data from Snow *et al.*⁴ matched to monthly temperature from CRU weather station data, summarized and smoothed using a generalized additive model. The observed optimum temperature (red dashed line) closely matches expectations based on laboratory experiments (grey dashed line). (C) Main panel regression estimate for prevalence response to temperature. The modeled optimum temperature (red dashed line) is slightly lower than in laboratory experiments (grey dashed line). (D) Histogram of optimum temperatures derived from 1,000 bootstrapped estimates of the panel regression model shown in panel (C). The mean optimum temperature across all bootstrap samples (red dashed line) is identical to the optimum shown in panel (C).

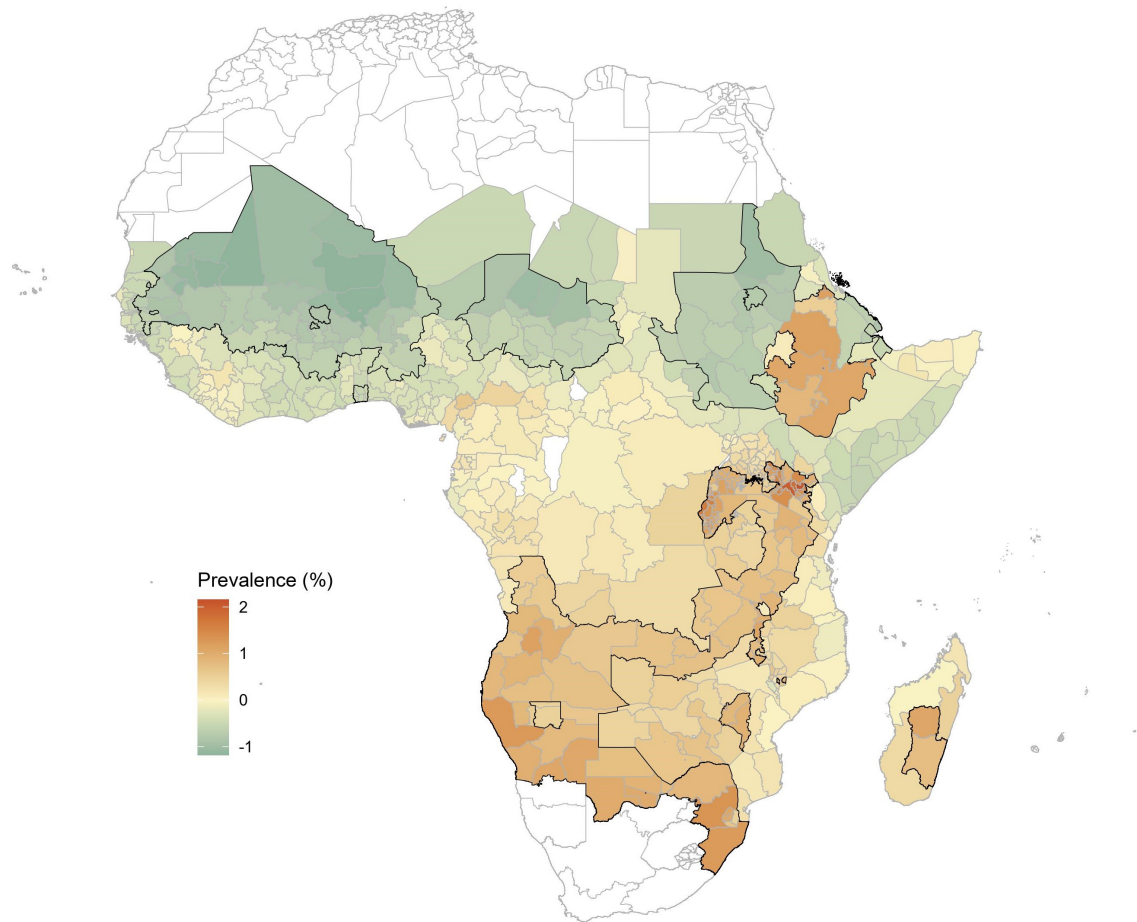


Figure S2: Historical changes in malaria prevalence attributable to anthropogenic climate change from 1901 to 2014. Map shows the estimated climate-driven change in prevalence (in percentage points) in a polygon based on the difference between the historical climate in 2010-2014 and a counterfactual scenario for the same period simulated without anthropogenic warming. Polygons with a black solid outline indicate areas with changes that were statistically significant ($\alpha = 0.05$) based on the sign of 10,000 simulations. Mean estimates shown here provide the same information as in Figure 3, but on a single color scale.

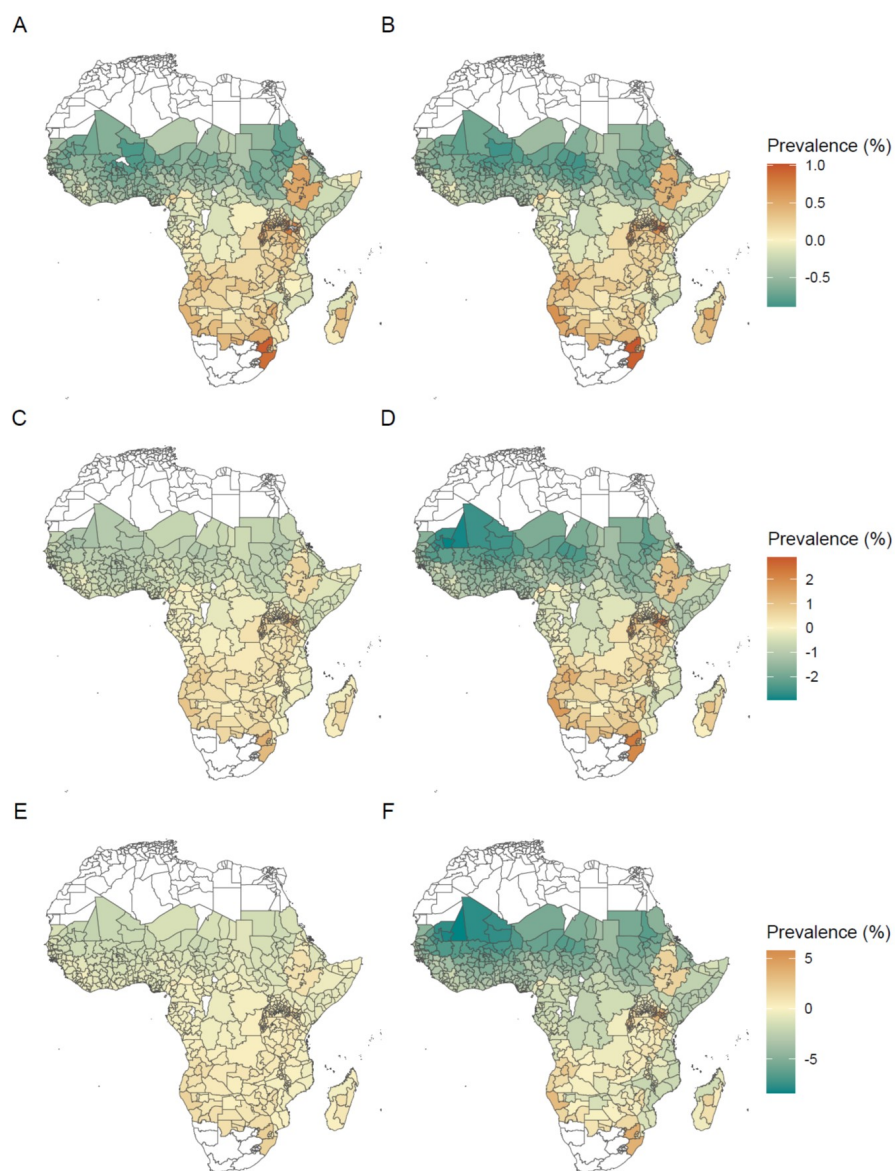


Figure S3: Projected future changes in malaria prevalence driven by climate change from 2015 to 2100. Maps show the estimated change in prevalence (in percentage points) in low-emissions (SSP1-RCP2.6; A,B), moderate-emissions (SSP2-RCP4.5; C,D), and high-emissions (SSP5-RCP8.5; E,F) scenarios, projected to mid-century (2048-2052; A,C,E) or the end of the century (2096-2100; B,D,F). Projections are reported as differences relative to a present-day baseline (2015-2020). Mean estimates in panel D provide the same information as in Figure 4, but on a single color scale (*i.e.*, no uncertainty visualization).

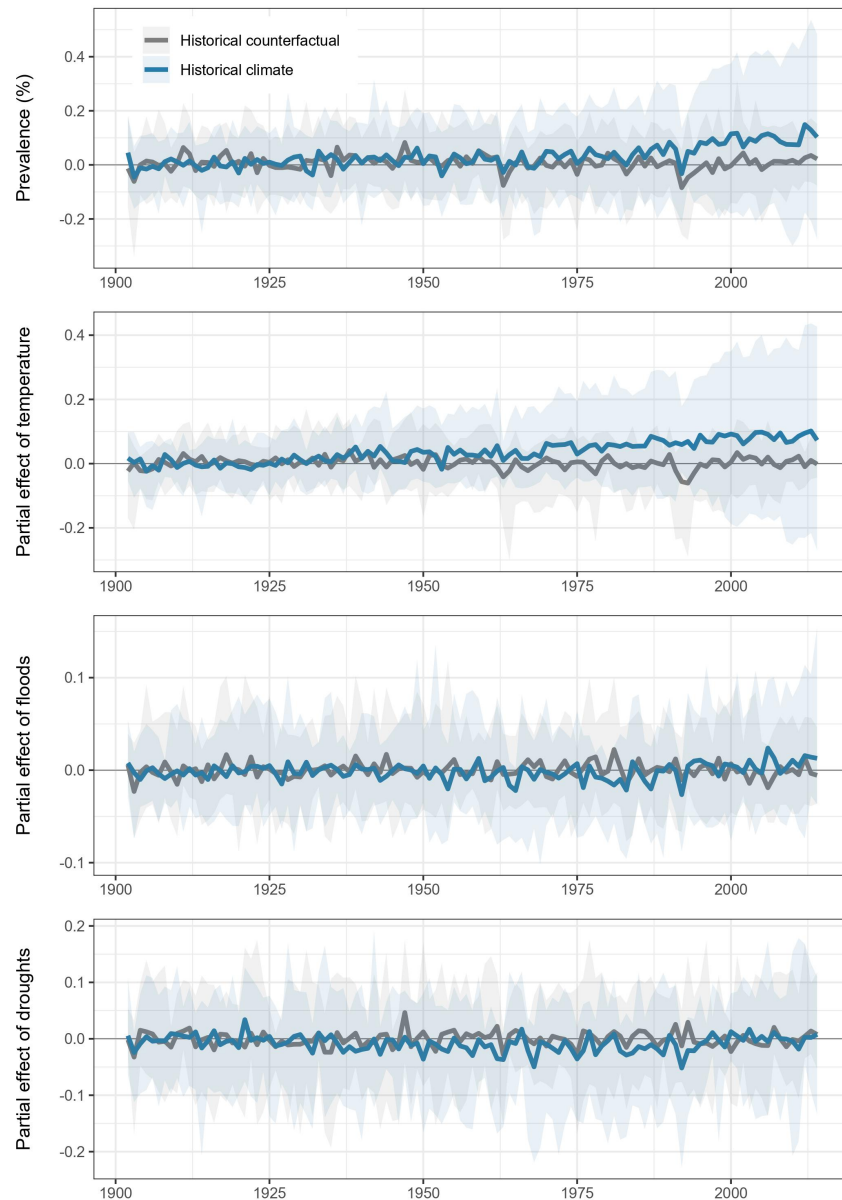


Figure S4: **Historical impacts of climate change decomposed by variable.** Partial predictions of changes in malaria attributable to anthropogenic climate change are made based on (A) temperature, (B) flood shocks, and (C) drought shocks. As in Figure 2, predictions based on true historical climate (blue) are compared to counterfactual predictions without anthropogenic warming (grey), relative to a 1901 to 1930 baseline. Thick lines are the median estimate across all 10,000 simulations; shading indicates 5% and 95% percentiles. Plots begin in 1902 with the first full year of predictions (due to lag effects).

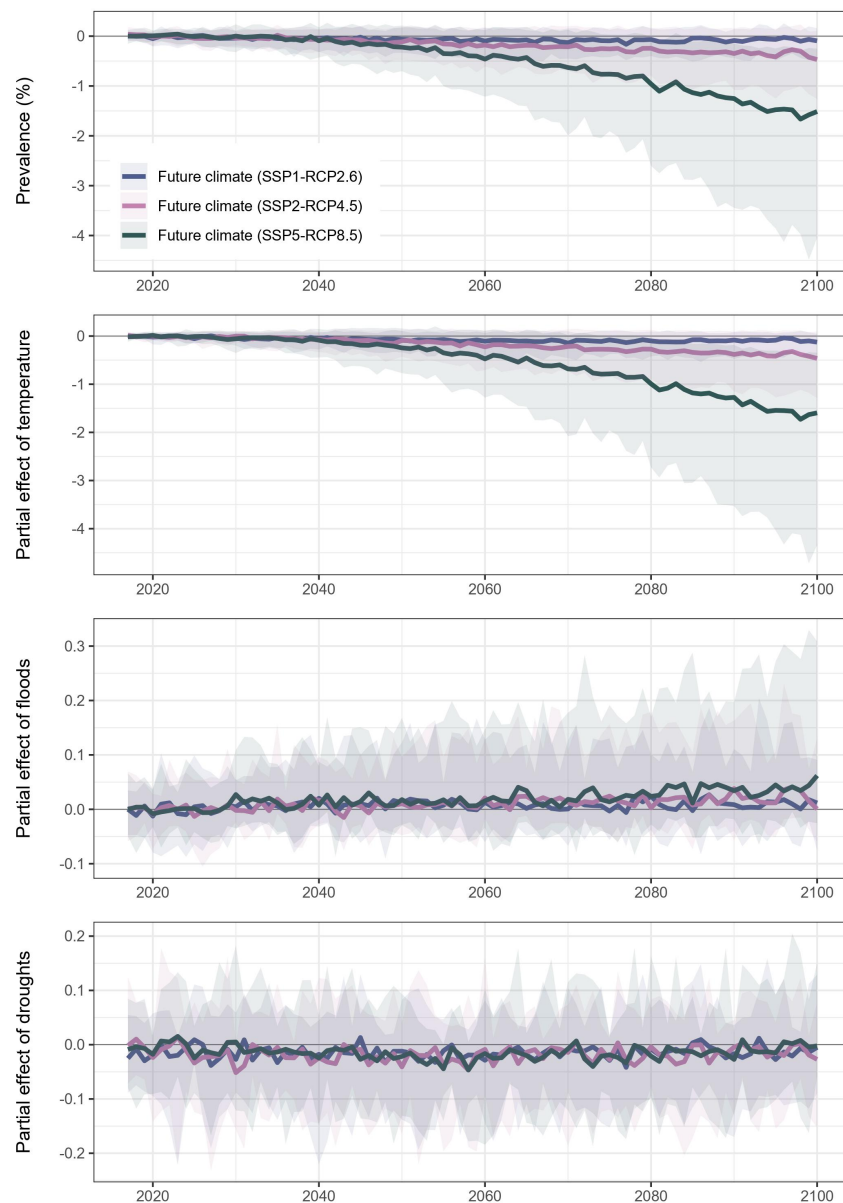


Figure S5: **Future impacts of climate change decomposed by variable.** Partial predictions of changes in malaria attributable to future climate change are made based on (A) temperature, (B) flood shocks, and (C) drought shocks. Projections are shown relative to the mean prevalence from 2015-2020, and as in Figure 2, line color indicates scenario (blue: SSP1-RCP2.6; pink: SSP2-RCP4.5; green: SSP5-RCP8.5). Thick lines are the median estimate across all 10,000 simulations; shading indicates 5% and 95% percentiles. Plots begin in 2016 with the first full year of predictions (due to lag effects).

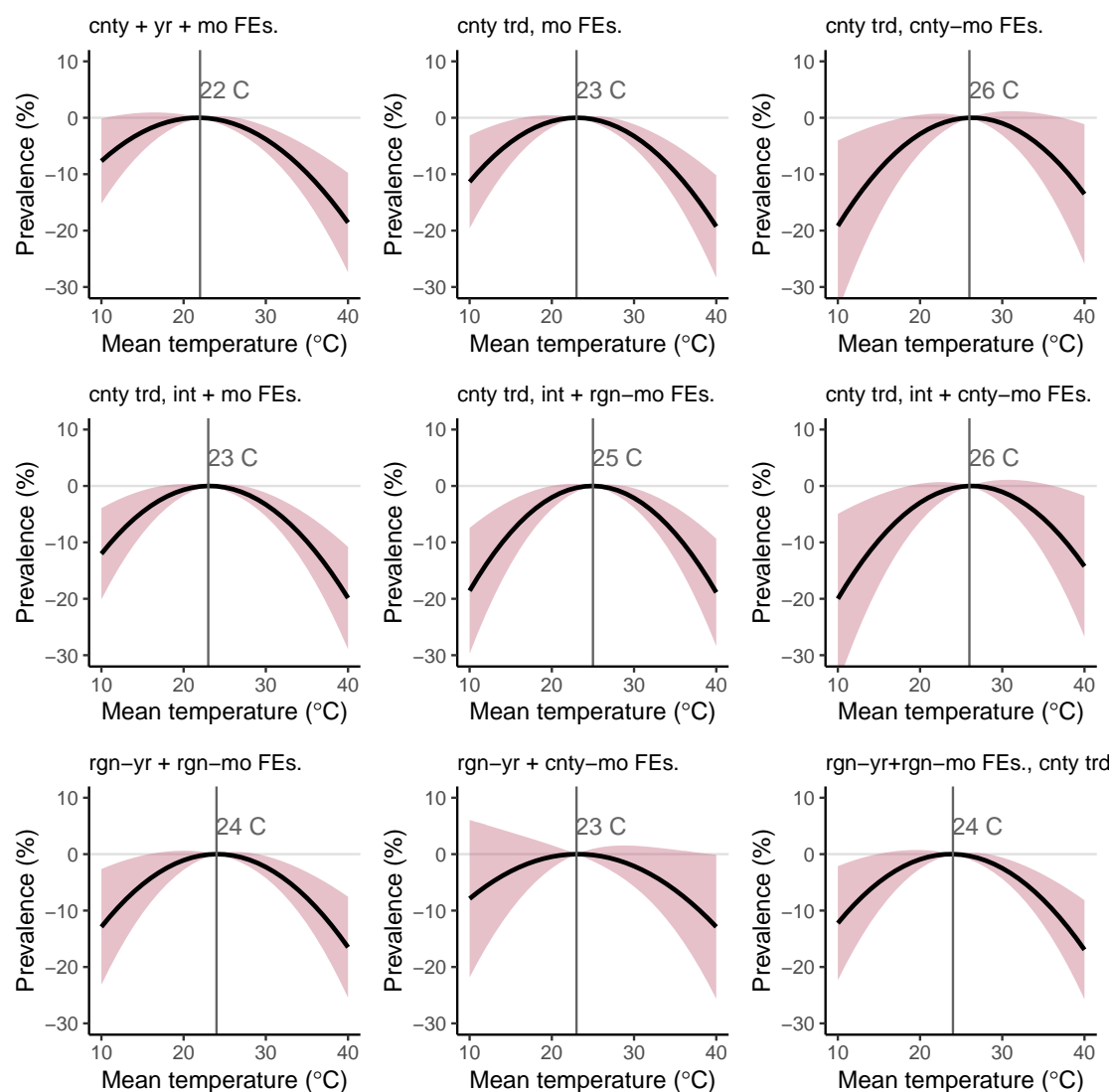


Figure S6: **Sensitivity of the $PfPR_{2-10}$ -temperature relationship to alternative spatiotemporal controls.** All panels show the estimated relationship between malaria prevalence for children aged 2-10 and monthly average temperature and all include fixed effects (i.e., dummy variables) at the scale of the first administrative unit (i.e., ADM1). All temperature responses are plotted relative to the model-specific temperature at which prevalence is maximized; this peak temperature is indicated in orange text and with a vertical orange line in each panel. From top-left to bottom-right, model controls are: country, year, and month fixed effects; country-specific quadratic time trends and month fixed effects; country-specific quadratic time trends and country-by-month fixed effects; country-specific quadratic time trends and intervention period and month fixed effects; country-specific quadratic time trends and intervention period and region-by-month fixed effects; country-specific quadratic time trends and intervention period and country-by-month fixed effects; region-by-year and region-by-month fixed effects; region-by-year and country-by-month fixed effects; and region-by-year and region-by-month fixed effects and country-specific linear time trends. The preferred specification used throughout the main text is the center panel, which includes country-specific quadratic time trends and intervention period and region-by-month fixed effects. In all panels, “region” refers to the Global Burden of Disease regional definitions of Western, Southern, Central, and Eastern Africa. All standard errors are clustered at the first administrative unit (e.g., province) level.

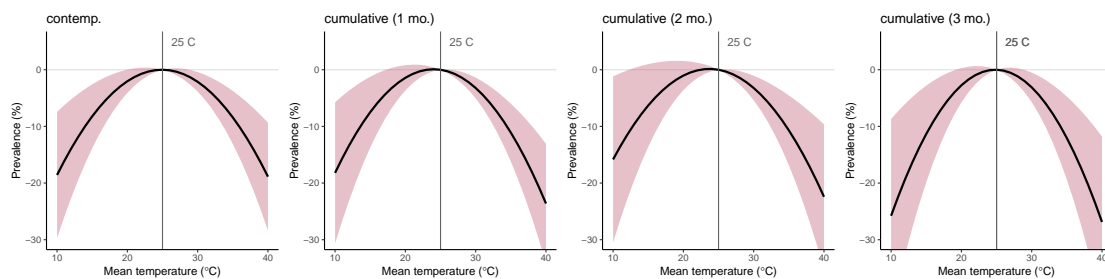


Figure S7: Cumulative effect of contemporaneous and lagged temperature on $PfPR_{2-10}$. All panels show the estimated relationship between malaria prevalence for children aged 2-10 and monthly average temperature and are plotted relative to a monthly average temperature of 25°C. The first panel shows the effect of monthly average temperature on the same month's average prevalence (this is the main estimate used throughout the main text). The second panel shows the cumulative effect of contemporaneous temperature and the prior month's temperature on prevalence, while the last two columns show analogous results for two and three months of lags, respectively. In all specifications, three months of lagged precipitation extremes are included, as well as all other controls shown in Equation 1. All standard errors are clustered at the first administrative unit (e.g., province) level.

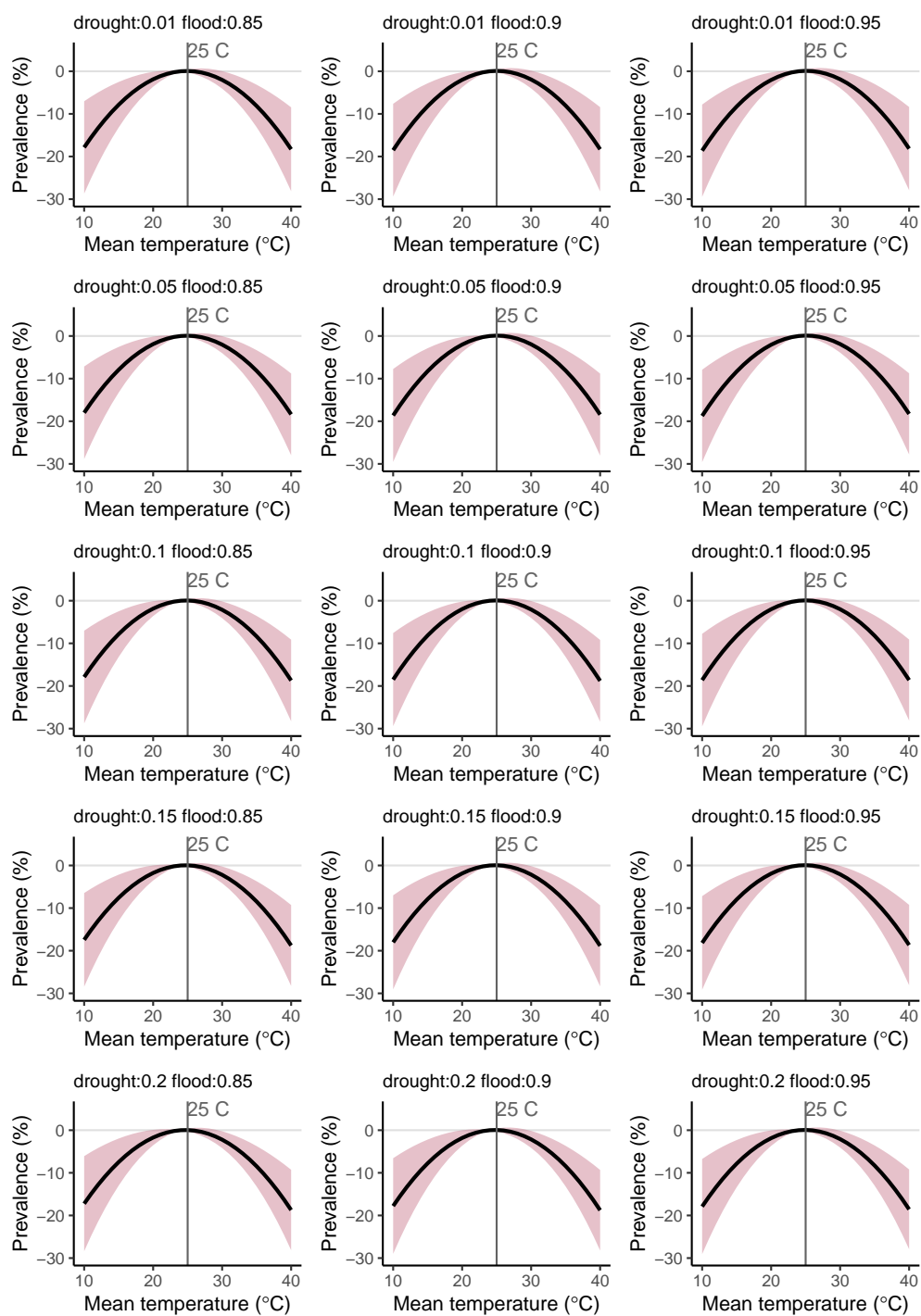


Figure S8: **Sensitivity of $PfPR_{2-10}$ -temperature relationship to alternative drought and flood definitions.** All panels show the estimated relationship between malaria prevalence for children aged 2-10 and monthly average temperature and are plotted relative to a monthly average temperature of 25°C. Cutoff values for drought and flood definitions are given in the titles of each panel. For example, the first panel in the upper left defines drought as monthly total precipitation that falls below 1% of the long-run location- and month-specific mean, and defines flood as monthly total precipitation that falls above 85% of the long-run location- and month-specific mean. In all specifications, three months of lagged precipitation extremes are included, as well as all other controls shown in Equation 1. The main specification used throughout the paper uses a drought cutoff of 10% and a flood cutoff of 90%. All standard errors are clustered at the first administrative unit (e.g., province) level.

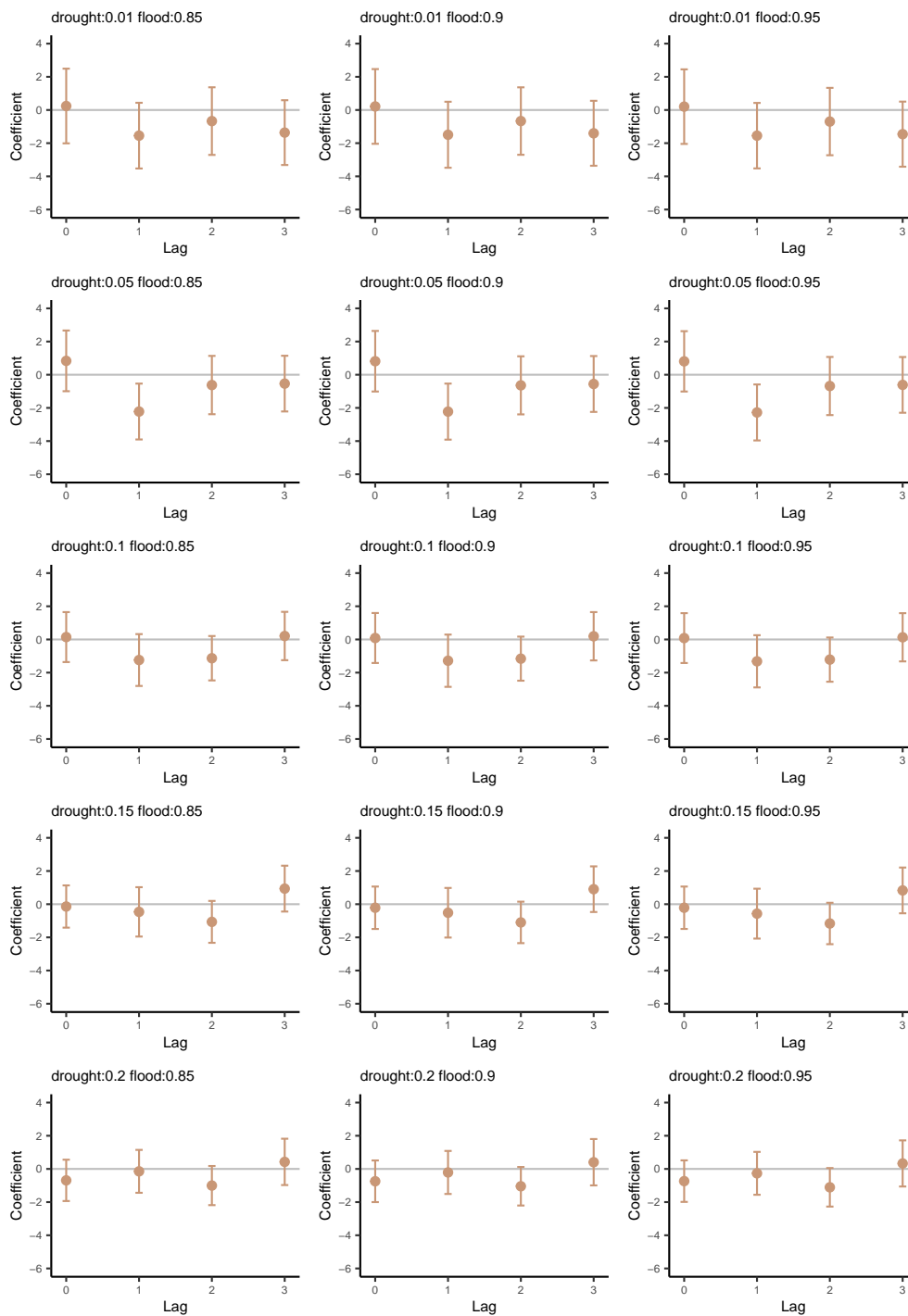


Figure S9: **Sensitivity of $PfPR_{2-10}$ -drought relationship to alternative drought and flood definitions.** All panels show the estimated relationship between malaria prevalence for children aged 2-10 and contemporaneous and lagged drought events. Point estimates are given by solid circles, while vertical bars indicate 95% confidence intervals. Cutoff values for drought and flood definitions are given in the titles of each panel. For example, the first panel in the upper left defines drought as monthly total precipitation that falls below 1% of the long-run location- and month-specific mean, and defines flood as monthly total precipitation that falls above 85% of the long-run location- and month-specific mean. In all specifications, three months of lagged precipitation extremes are included, as well as all other controls shown in Equation 1. The main specification used throughout the paper uses a drought cutoff of 10% and a flood cutoff of 90%. All standard errors are clustered at the first administrative unit (e.g., province) level.

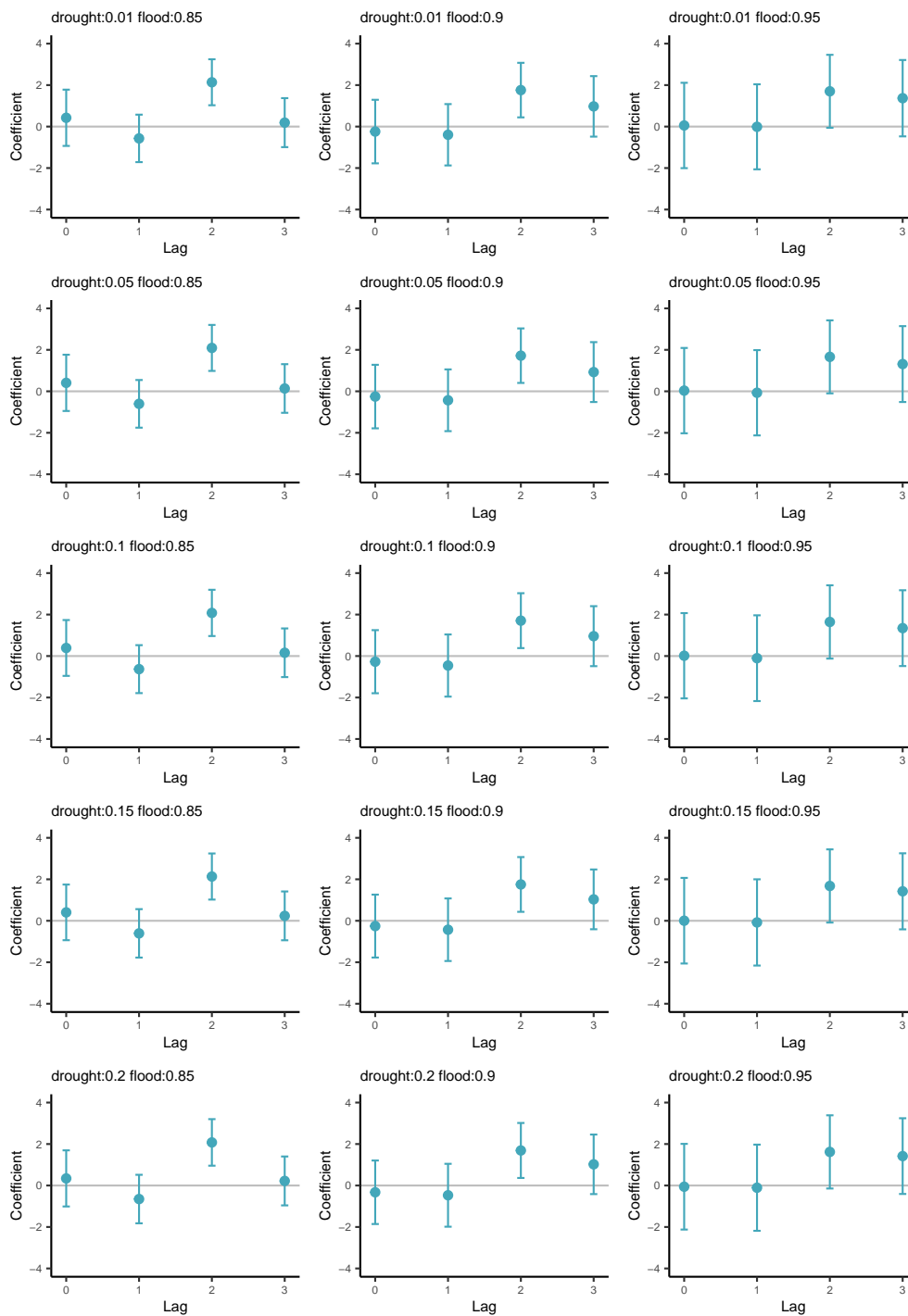


Figure S10: **Sensitivity of $PfPR_{2-10}$ -flood relationship to alternative drought and flood definitions.** All panels show the estimated relationship between malaria prevalence for children aged 2-10 and contemporaneous and lagged flood events. Point estimates are given by solid circles, while vertical bars indicate 95% confidence intervals. Cutoff values for drought and flood definitions are given in the titles of each panel. For example, the first panel in the upper left defines drought as monthly total precipitation that falls below 1% of the long-run location- and month-specific mean, and defines flood as monthly total precipitation that falls above 85% of the long-run location- and month-specific mean. In all specifications, three months of lagged precipitation extremes are included, as well as all other controls shown in Equation 1. The main specification used throughout the paper uses a drought cutoff of 10% and a flood cutoff of 90%. All standard errors are clustered at the first administrative unit (e.g., province) level.

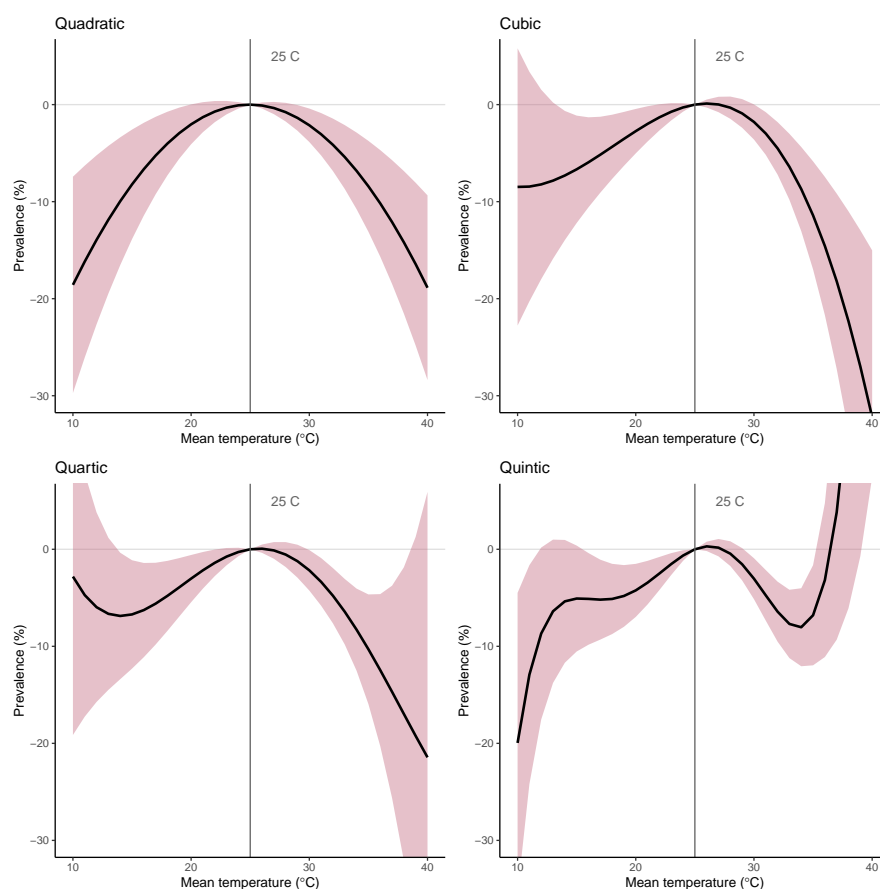


Figure S11: **Alternative functional forms for the $PfPR_{2-10}$ -temperature relationship.** All panels show the estimated relationship between malaria prevalence for children aged 2-10 and monthly average temperature and are plotted relative to a monthly average temperature of 25°C. Starting in the upper left, the first panel shows the paper's main specification, a quadratic functional form for the prevalence-temperature relationship. The second panel shows a cubic functional form, the third a quartic, and the fourth a quintic. **All standard errors are clustered at the first administrative unit (e.g., province) level.**

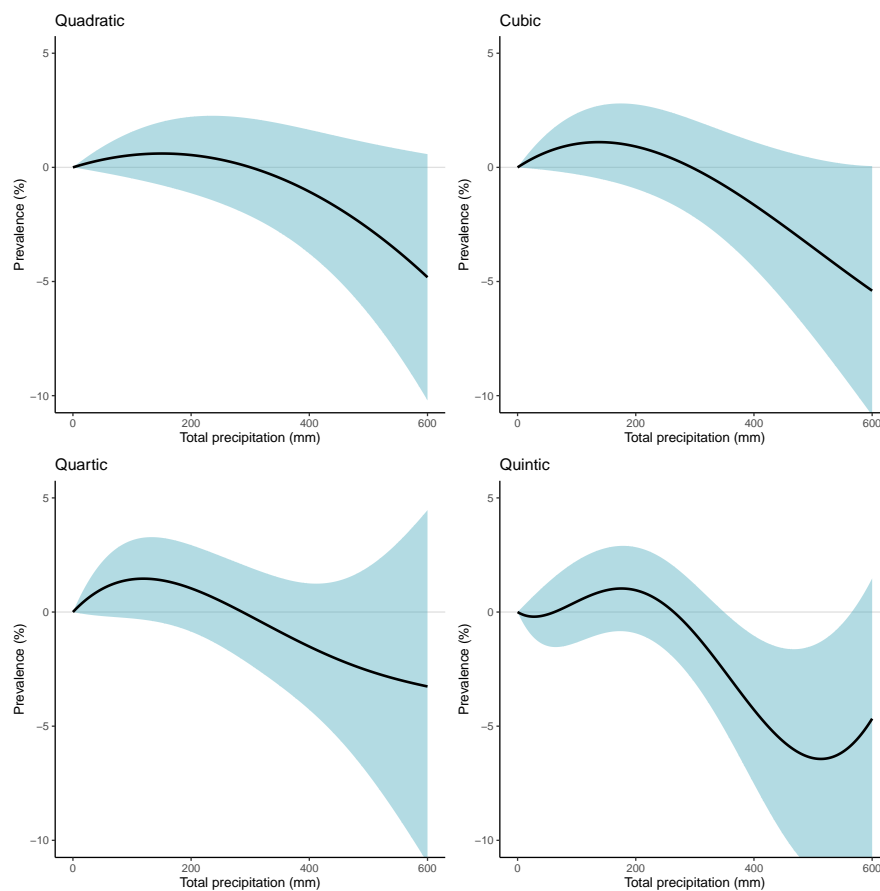


Figure S12: **Non-linearities in the $PfPR_{2-10}$ -precipitation relationship.** All panels show the estimated relationship between malaria prevalence for children aged 2-10 and monthly cumulative precipitation and are plotted relative to a month with no rainfall. All relationships are estimated for contemporaneous monthly precipitation. All standard errors are clustered at the first administrative unit (e.g., province) level.

Region	Scenario	2048-2052		2096-2100	
		Estimate	95% CI	Estimate	95% CI
Sub-Saharan Africa (continent-wide)	SSP1-RCP2.6	-0.0828	(-0.402, 0.169)	-0.0891	(-0.487, 0.165)
	SSP2-RCP4.5	-0.136	(-0.543, 0.204)	-0.398	(-1.26, 0.251)
	SSP5-RCP8.5	-0.234	(-0.794, 0.264)	-1.75	(-4.61, -0.0332)
East Africa	SSP1-RCP2.6	0.114	(-0.174, 0.466)	0.102	(-0.243, 0.454)
	SSP2-RCP4.5	0.138	(-0.244, 0.542)	0.142	(-0.536, 0.830)
	SSP5-RCP8.5	0.163	(-0.370, 0.700)	-0.483	(-2.44, 0.981)
Central Africa	SSP1-RCP2.6	-0.0284	(-0.353, 0.215)	-0.0557	(-0.405, 0.249)
	SSP2-RCP4.5	-0.00663	(-0.463, 0.399)	-0.179	(-1.05, 0.535)
	SSP5-RCP8.5	-0.0823	(-0.651, 0.457)	-1.23	(-3.91, 0.432)
Southern Africa	SSP1-RCP2.6	0.318	(-0.102, 0.833)	0.342	(-0.0654, 0.931)
	SSP2-RCP4.5	0.481	(-0.0720, 1.04)	0.838	(-0.152, 1.90)
	SSP5-RCP8.5	0.838	(-0.0779, 1.81)	0.621	(-2.19, 2.62)
West Africa	SSP1-RCP2.6	-0.443	(-0.936, -0.132)	-0.441	(-1.08, 0.105)
	SSP2-RCP4.5	-0.669	(-1.28, -0.222)	-1.44	(-2.87, -0.464)
	SSP5-RCP8.5	-1.03	(-1.86, -0.354)	-4.09	(-8.75, -1.48)

Table S1: **Projected future impacts of climate change on $PfPR_{2-10}$.** Estimates and confidence intervals are all given as percentage point changes from a 2015-2020 baseline, estimated across 10,000 simulations.

	<i>Dependent variable:</i>								
	$PfPR_{2-10}$								
	city + yr + mo FEs. (1)	city trd, mo FEs. (2)	city trd, city-mo FEs. (3)	city trd, int + mo FEs. (4)	city trd, int + rgn-mo FEs. (5)	city trd, rgn-mo FEs. (6)	city + yr + city-mo FEs. (7)	city + yr + city-mo FEs. (8)	city + yr + city-mo FEs. (9)
Avg temp. (°C)	2.42*** (0.83)	3.08*** (0.88)	3.80*** (1.39)	3.23*** (0.87)	4.15*** (1.08)	3.97*** (1.39)	3.13*** (1.00)	2.11 (1.34)	3.06*** (0.99)
Avg temp.2 (°C)	-0.06*** (0.02)	-0.07*** (0.02)	-0.07*** (0.03)	-0.07*** (0.02)	-0.08*** (0.02)	-0.08*** (0.03)	-0.07*** (0.02)	-0.05* (0.03)	-0.06*** (0.02)
Flood	-0.76 (0.75)	-0.37 (0.74)	-0.73 (0.82)	-0.27 (0.74)	-0.27 (0.78)	-0.65 (0.82)	-0.88 (0.76)	-1.15 (0.80)	-0.82 (0.74)
Flood (lag 1)	-0.56 (0.73)	-0.40 (0.76)	-0.50 (0.85)	-0.46 (0.75)	-0.46 (0.76)	-0.55 (0.83)	-0.77 (0.73)	-1.09 (0.80)	-0.57 (0.72)
Flood (lag 2)	1.68*** (0.65)	1.52*** (0.65)	2.03*** (0.72)	1.69*** (0.65)	1.71** (0.68)	2.19*** (0.72)	2.13*** (0.68)	1.94*** (0.72)	1.79*** (0.67)
Flood (lag 3)	0.58 (0.69)	0.90 (0.71)	1.89** (0.80)	0.87 (0.71)	0.96 (0.74)	1.91** (0.81)	0.08 (0.70)	0.74 (0.77)	0.38 (0.68)
Drought	0.56 (0.81)	0.87 (0.74)	-0.48 (0.82)	0.84 (0.74)	0.09 (0.77)	-0.57 (0.83)	-0.35 (0.81)	-0.69 (0.86)	-0.13 (0.74)
Drought (lag 1)	-1.01 (0.75)	-1.02 (0.77)	-1.39 (0.86)	-0.92 (0.78)	-1.28 (0.80)	-1.34 (0.86)	-1.62** (0.76)	-1.28 (0.85)	-1.33* (0.77)
Drought (lag 2)	-0.97 (0.68)	-1.08* (0.65)	-0.88 (0.76)	-1.04 (0.65)	-1.16* (0.68)	-0.95 (0.76)	-1.18* (0.69)	-0.85 (0.77)	-1.24* (0.67)
Drought (lag 3)	0.06 (0.71)	0.16 (0.73)	0.36 (0.81)	0.06 (0.73)	0.19 (0.74)	0.15 (0.80)	-0.06 (0.77)	0.11 (0.83)	-0.16 (0.75)
Intvn. 1955-69					-4.80*** (1.27)	-5.01*** (1.35)			
Intvn. 2000-15					-3.35** (1.61)	-3.88** (1.64)			
Observations	9,875	9,875	9,875	9,875	9,875	9,875	9,875	9,875	9,875
R ²	0.52	0.52	0.56	0.53	0.53	0.57	0.56	0.60	0.59
Adjusted R ²	0.48	0.49	0.51	0.49	0.49	0.51	0.52	0.53	0.54

Table S2: Sensitivity of estimated effects of temperature and rainfall on $PfPR_{2-10}$ to alternative spatiotemporal controls. All columns show regression results for a dependent variable of malaria prevalence for children aged 2-10 ($PfPR_{2-10}$). All include fixed effects (i.e., dummy variables) at the scale of the first administrative unit (i.e., ADM1). Other model controls by column are: (1) country, year, and month fixed effects; (2) country-specific quadratic time trends and month fixed effects; (3) country-specific quadratic time trends and country-by-month fixed effects; (4) country-specific quadratic time trends and intervention period and month fixed effects; (5) country-specific quadratic time trends and intervention period and region-by-month fixed effects; (6) country-specific quadratic time trends and intervention period and country-by-month fixed effects; (7) region-by-year and region-by-month fixed effects; (8) region-by-year and country-by-month fixed effects; (9) and region-by-year and region-by-month fixed effects and country-specific linear time trends. The preferred specification used throughout the main text is column (5). In columns (5) and (7)-(9), "region" refers to the Global Burden of Disease regional definitions of Western, Southern, Central, and Eastern Africa. All standard errors are clustered at the first administrative unit (e.g., province) level.

549 References

- 550 1. Ebi, K. L, Åström, C, Boyer, C. J, Harrington, L. J, Hess, J. J, Honda, Y, Kazura, E,
551 Stuart-Smith, R. F, & Otto, F. E. (2020) Using detection and attribution to quantify
552 how climate change is affecting health: Study explores detection and attribution to
553 examine how climate change is affecting health. *Health Affairs* **39**, 2168–2174.
- 554 2. Carlson, C. J, Alam, M. S, North, M. A, Onyango, E, & Stewart-Ibarra, A. M.
555 (2023) The health burden of climate change: a call for global scientific action. *PLOS*
556 *Climate* **2**, e0000126.
- 557 3. Romanello, M, Di Napoli, C, Drummond, P, Green, C, Kennard, H, Lampard, P,
558 Scamman, D, Arnell, N, Ayeb-Karlsson, S, Ford, L. B, et al. (2022) The 2022 report
559 of the lancet countdown on health and climate change: health at the mercy of fossil
560 fuels. *The Lancet* **400**, 1619–1654.
- 561 4. Snow, R. W, Sartorius, B, Kyalo, D, Maina, J, Amratia, P, Mundia, C. W, Bejon,
562 P, & Noor, A. M. (2017) The prevalence of *Plasmodium falciparum* in sub-Saharan
563 Africa since 1900. *Nature* **550**, 515–518.
- 564 5. Alcayna, T, Fletcher, I, Gibb, R, Tremblay, L, Funk, S, Rao, B, & Lowe, R. (2022)
565 Climate-sensitive disease outbreaks in the aftermath of extreme climatic events: a
566 scoping review. *One Earth* **5**, 336–350.
- 567 6. Mordecai, E. A, Paaijmans, K. P, Johnson, L. R, Balzer, C, Ben-Horin, T, de Moor,
568 E, McNally, A, Pawar, S, Ryan, S. J, Smith, T. C, et al. (2013) Optimal temperature
569 for malaria transmission is dramatically lower than previously predicted. *Ecology*
570 *Letters* **16**, 22–30.
- 571 7. Mordecai, E. A, Caldwell, J. M, Grossman, M. K, Lippi, C. A, Johnson, L. R, Neira,
572 M, Rohr, J. R, Ryan, S. J, Savage, V, Shocket, M. S, et al. (2019) Thermal biology
573 of mosquito-borne disease. *Ecology Letters* **22**, 1690–1708.
- 574 8. Villena, O. C, Ryan, S. J, Murdock, C. C, & Johnson, L. R. (2022) Temperature
575 impacts the environmental suitability for malaria transmission by *Anopheles gambiae*
576 and *Anopheles stephensi*. *Ecology* p. e3685.
- 577 9. Ryan, S. J, McNally, A, Johnson, L. R, Mordecai, E. A, Ben-Horin, T, Paaijmans,
578 K, & Lafferty, K. D. (2015) Mapping physiological suitability limits for malaria in
579 Africa under climate change. *Vector-Borne and Zoonotic Diseases* **15**, 718–725.
- 580 10. Ryan, S. J, Lippi, C. A, & Zermoglio, F. (2020) Shifting transmission risk for malaria
581 in Africa with climate change: a framework for planning and intervention. *Malaria*
582 *Journal* **19**, 1–14.
- 583 11. Caminade, C, McIntyre, K. M, & Jones, A. E. (2019) Impact of recent and future cli-
584 mate change on vector-borne diseases. *Annals of the New York Academy of Sciences*
585 **1436**, 157–173.

- 586 12. Murdock, C, Sternberg, E, & Thomas, M. (2016) Malaria transmission potential
587 could be reduced with current and future climate change. *Scientific Reports* **6**, 1–7.
- 588 13. Yamana, T. K, Bomblies, A, & Eltahir, E. A. (2016) Climate change unlikely to
589 increase malaria burden in West Africa. *Nature Climate Change* **6**, 1009–1013.
- 590 14. Loevinsohn, M. E. (1994) Climatic warming and increased malaria incidence in
591 rwanda. *The Lancet* **343**, 714–718.
- 592 15. Ezzati, M, Lopez, A. D, Rodgers, A. A, & Murray, C. J. (2004) *Comparative quan-*
593 *tification of health risks: global and regional burden of disease attributable to selected*
594 *major risk factors*. (World Health Organization).
- 595 16. Hay, S. I, Rogers, D. J, Randolph, S. E, Stern, D. I, Cox, J, Shanks, G. D, & Snow,
596 R. W. (2002) Hot topic or hot air? Climate change and malaria resurgence in East
597 African highlands. *Trends in Parasitology* **18**, 530–534.
- 598 17. Alsop, Z. (2007) Malaria returns to Kenya’s highlands as temperatures rise. *The*
599 *Lancet* **370**, 925–926.
- 600 18. Shanks, G. D, Hay, S. I, Omumbo, J. A, & Snow, R. W. (2005) Malaria in kenya’s
601 western highlands. *Emerging infectious diseases* **11**, 1425.
- 602 19. Gething, P. W, Smith, D. L, Patil, A. P, Tatem, A. J, Snow, R. W, & Hay, S. I.
603 (2010) Climate change and the global malaria recession. *Nature* **465**, 342–345.
- 604 20. Zhou, G, Minakawa, N, Githeko, A. K, & Yan, G. (2004) Association between climate
605 variability and malaria epidemics in the east african highlands. *Proceedings of the*
606 *National Academy of Sciences* **101**, 2375–2380.
- 607 21. Pascual, M, Ahumada, J. A, Chaves, L. F, Rodo, X, & Bouma, M. (2006) Malaria
608 resurgence in the East African highlands: temperature trends revisited. *Proceedings*
609 *of the National Academy of Sciences* **103**, 5829–5834.
- 610 22. Pascual, M, Cazelles, B, Bouma, M, Chaves, L, & Koelle, K. (2008) Shifting patterns:
611 malaria dynamics and rainfall variability in an african highland. *Proceedings of the*
612 *Royal Society B: Biological Sciences* **275**, 123–132.
- 613 23. Omumbo, J. A, Lyon, B, Waweru, S. M, Connor, S. J, & Thomson, M. C. (2011)
614 Raised temperatures over the kericho tea estates: revisiting the climate in the east
615 african highlands malaria debate. *Malaria Journal* **10**, 1–16.
- 616 24. Alonso, D, Bouma, M. J, & Pascual, M. (2010) Epidemic malaria and warmer
617 temperatures in recent decades in an East African highland. *Proceedings of the*
618 *Royal Society B: Biological Sciences* **278**, 1661–1669.

- 619 25. Hay, S. I, Myers, M. F, Burke, D. S, Vaughn, D. W, Endy, T, Ananda, N, Shanks,
620 G. D, Snow, R. W, & Rogers, D. J. (2000) Etiology of interepidemic periods of
621 mosquito-borne disease. *Proceedings of the National Academy of Sciences* **97**, 9335–
622 9339.
- 623 26. Shanks, G, Biomndo, K, Hay, S, & Snow, R. (2000) Changing patterns of clinical
624 malaria since 1965 among a tea estate population located in the kenyan highlands.
625 *Transactions of the Royal Society of Tropical Medicine and Hygiene* **94**, 253–255.
- 626 27. Shanks, G. D, Hay, S. I, Stern, D. I, Biomndo, K, & Snow, R. W. (2002) Meteorologic
627 influences on plasmodium falciparum malaria in the highland tea estates of kericho,
628 western kenya. *Emerging infectious diseases* **8**, 1404.
- 629 28. Hay, S. I, Cox, J, Rogers, D. J, Randolph, S. E, Stern, D. I, Shanks, G. D, Myers,
630 M. F, & Snow, R. W. (2002) Climate change and the resurgence of malaria in the
631 East African highlands. *Nature* **415**, 905.
- 632 29. Hay, S. I, Shanks, G. D, Stern, D. I, Snow, R. W, Randolph, S. E, & Rogers, D. J.
633 (2005) Climate variability and malaria epidemics in the highlands of east africa.
634 *Trends in parasitology* **21**, 52–53.
- 635 30. Stern, D. I, Gething, P. W, Kabaria, C. W, Temperley, W. H, Noor, A. M, Okiro,
636 E. A, Shanks, G. D, Snow, R. W, & Hay, S. I. (2011) Temperature and malaria
637 trends in highland east africa. *PloS one* **6**, e24524.
- 638 31. Krsulovic, F. A. M, Moulton, T. P, Lima, M, & Jacksic, F. (2021) Epidemic malaria
639 dynamics in eastern africa highlands: the role of climate change and human popula-
640 tion growth. *Ecol Evolut Bio* **6**, 23–30.
- 641 32. Chaves, L. F & Koenraad, C. J. (2010) Climate change and highland malaria: fresh
642 air for a hot debate. *The Quarterly review of biology* **85**, 27–55.
- 643 33. Siraj, A, Santos-Vega, M, Bouma, M, Yadeta, D, Carrascal, D. R, & Pascual, M.
644 (2014) Altitudinal changes in malaria incidence in highlands of Ethiopia and Colom-
645 bia. *Science* **343**, 1154–1158.
- 646 34. Rodó, X, Martinez, P. P, Siraj, A, & Pascual, M. (2021) Malaria trends in Ethiopian
647 highlands track the 2000 ‘slowdown’ in global warming. *Nature Communications* **12**,
648 1–12.
- 649 35. Ruiz, D, Brun, C, Connor, S. J, Omumbo, J. A, Lyon, B, & Thomson, M. C. (2014)
650 Testing a multi-malaria-model ensemble against 30 years of data in the kenyan high-
651 lands. *Malaria Journal* **13**, 1–14.
- 652 36. Pörtner, H.-O, Roberts, D. C, Adams, H, Adler, C, Aldunce, P, Ali, E, Begum, R. A,
653 Betts, R, Kerr, R. B, Biesbroek, R, et al. (2022) *Climate Change 2022: Impacts,*
654 *adaptation and vulnerability*. (IPCC Geneva, Switzerland:).

- 655 37. Callahan, C. W & Mankin, J. S. (2022) National attribution of historical climate
656 damages. *Climatic Change* **172**, 40.
- 657 38. Swain, D. L, Singh, D, Touma, D, & Diffenbaugh, N. S. (2020) Attributing extreme
658 events to climate change: a new frontier in a warming world. *One Earth* **2**, 522–527.
- 659 39. Stott, P. A, Christidis, N, Otto, F. E, Sun, Y, Vanderlinden, J.-P, van Oldenborgh,
660 G. J, Vautard, R, von Storch, H, Walton, P, Yiou, P, et al. (2016) Attribution of ex-
661 treme weather and climate-related events. *Wiley Interdisciplinary Reviews: Climate*
662 *Change* **7**, 23–41.
- 663 40. Otto, F. E. (2017) Attribution of weather and climate events. *Annual Review of*
664 *Environment and Resources* **42**, 627–646.
- 665 41. Ebi, K. L, Ogden, N. H, Semenza, J. C, & Woodward, A. (2017) Detecting and
666 attributing health burdens to climate change. *Environmental Health Perspectives*
667 **125**, 085004.
- 668 42. Burke, M, González, F, Baylis, P, Heft-Neal, S, Baysan, C, Basu, S, & Hsiang, S.
669 (2018) Higher temperatures increase suicide rates in the United States and Mexico.
670 *Nature Climate Change* **8**, 723–729.
- 671 43. Carleton, T. A & Hsiang, S. M. (2016) Social and economic impacts of climate.
672 *Science* **353**.
- 673 44. Organization, W. H et al. (2022) *World malaria report 2022*. (World Health Orga-
674 nization).
- 675 45. Carleton, T. A. (2017) Crop-damaging temperatures increase suicide rates in India.
676 *Proceedings of the National Academy of Sciences* **114**, 8746–8751.
- 677 46. Carleton, T, Jina, A, Delgado, M, Greenstone, M, Houser, T, Hsiang, S, Hultgren,
678 A, Kopp, R. E, McCusker, K. E, Nath, I, et al. (2022) Valuing the global mortality
679 consequences of climate change accounting for adaptation costs and benefits. *The*
680 *Quarterly Journal of Economics* **137**, 2037–2105.
- 681 47. Adeola, A. M, Botai, J. O, Rautenbach, H, Adisa, O. M, Ncongwane, K. P, Botai,
682 C. M, & Adebayo-Ojo, T. C. (2017) Climatic variables and malaria morbidity in
683 mutale local municipality, south africa: a 19-year data analysis. *International journal*
684 *of environmental research and public health* **14**, 1360.
- 685 48. Lindsay, S. W, Bødker, R, Malima, R, Msangeni, H. A, & Kisinza, W. (2000) Effect
686 of 1997–98 el niño on highland malaria in tanzania. *The Lancet* **355**, 989–990.
- 687 49. Teklehaimanot, H. D, Lipsitch, M, Teklehaimanot, A, & Schwartz, J. (2004) Weather-
688 based prediction of plasmodium falciparum malaria in epidemic-prone regions of
689 ethiopia i. patterns of lagged weather effects reflect biological mechanisms. *Malaria*
690 *journal* **3**, 1–11.

- 691 50. Boyce, R, Reyes, R, Matte, M, Ntaro, M, Mulogo, E, Metlay, J. P, Band, L, & Sied-
692 ner, M. J. (2016) Severe flooding and malaria transmission in the western ugandan
693 highlands: implications for disease control in an era of global climate change. *The*
694 *Journal of infectious diseases* **214**, 1403–1410.
- 695 51. Paaijmans, K. P, Wandago, M. O, Githeko, A. K, & Takken, W. (2007) Unexpected
696 high losses of anopheles gambiae larvae due to rainfall. *PloS one* **2**, e1146.
- 697 52. Govoetchan, R, Gnanguenon, V, Azondékon, R, Agossa, R. F, Sovi, A, Oké-Agbo, F,
698 Ossè, R, & Akogbéto, M. (2014) Evidence for perennial malaria in rural and urban
699 areas under the sudanian climate of kandi, northeastern benin. *Parasites & Vectors*
700 **7**, 1–12.
- 701 53. Smith, M, Macklin, M, & Thomas, C. (2013) Hydrological and geomorphological
702 controls of malaria transmission. *Earth-Science Reviews* **116**, 109–127.
- 703 54. Mouchet, J, Manguin, S, Sircoulon, J, Laventure, S, Faye, O, Onapa, A, Carnevale,
704 P, Julvez, J, & Fontenille, D. (1998) Evolution of malaria in africa for the past 40
705 years: impact of climatic and human factors. *Journal of the American Mosquito*
706 *Control Association* **14**, 121–130.
- 707 55. Schultz, K. A & Mankin, J. S. (2019) Is temperature exogenous? the impact of civil
708 conflict on the instrumental climate record in sub-saharan africa. *American Journal*
709 *of Political Science* **63**, 723–739.
- 710 56. Auffhammer, M, Hsiang, S. M, Schlenker, W, & Sobel, A. (2011) Global climate
711 models and climate data: a user guide for economists. *Unpublished manuscript* **1**,
712 10529–10530.
- 713 57. Masson-Delmotte, V, Zhai, P, Pirani, A, Connors, S. L, Péan, C, Berger, S, Caud,
714 N, Chen, Y, Goldfarb, L, Gomis, M, et al. (2021) Climate change 2021: the physical
715 science basis.
- 716 58. Mordecai, E. A, Ryan, S. J, Caldwell, J. M, Shah, M. M, & LaBeaud, A. D. (2020)
717 Climate change could shift disease burden from malaria to arboviruses in africa. *The*
718 *Lancet Planetary Health* **4**, e416–e423.
- 719 59. Feachem, R. G, Chen, I, Akbari, O, Bertozzi-Villa, A, Bhatt, S, Binka, F, Boni,
720 M. F, Buckee, C, Dieleman, J, Dondorp, A, et al. (2019) Malaria eradication within
721 a generation: ambitious, achievable, and necessary. *The Lancet* **394**, 1056–1112.
- 722 60. Tian, H, Li, N, Li, Y, Kraemer, M. U, Tan, H, Liu, Y, Li, Y, Wang, B, Wu, P,
723 Cazelles, B, et al. (2022) Malaria elimination on Hainan Island despite climate
724 change. *Communications Medicine* **2**, 1–9.
- 725 61. Jaramillo-Ochoa, R, Sippy, R, Farrell, D. F, Cueva-Aponte, C, Beltrán-Ayala, E,
726 Gonzaga, J. L, Ordoñez-León, T, Quintana, F. A, Ryan, S. J, & Stewart-Ibarra,

- 727 A. M. (2019) Effects of political instability in Venezuela on malaria resurgence at
728 Ecuador–Peru border, 2018. *Emerging Infectious Diseases* **25**, 834.
- 729 62. Walker, P. G, White, M. T, Griffin, J. T, Reynolds, A, Ferguson, N. M, & Ghani,
730 A. C. (2015) Malaria morbidity and mortality in Ebola-affected countries caused by
731 decreased health-care capacity, and the potential effect of mitigation strategies: a
732 modelling analysis. *The Lancet Infectious Diseases* **15**, 825–832.
- 733 63. Miazgowicz, K, Shocket, M, Ryan, S, Villena, O, Hall, R, Owen, J, Adanlawo, T,
734 Balaji, K, Johnson, L, Mordecai, E, et al. (2020) Age influences the thermal suitability
735 of *Plasmodium falciparum* transmission in the Asian malaria vector *Anopheles*
736 *stephensi*. *Proceedings of the Royal Society B* **287**, 20201093.
- 737 64. Sinka, M, Pironon, S, Massey, N, Longbottom, J, Hemingway, J, Moyes, C, & Willis,
738 K. (2020) A new malaria vector in africa: Predicting the expansion range of anopheles
739 stephensi and identifying the urban populations at risk. *Proceedings of the National*
740 *Academy of Sciences* **117**, 24900–24908.
- 741 65. Ryan, S. J, Lippi, C. A, Villena, O. C, Singh, A. H, Murdock, C. C, & Johnson,
742 L. R. (2022) Mapping current and future thermal limits to suitability for malaria
743 transmission by the invasive mosquito anopheles stephensi. *bioRxiv* pp. 2022–12.
- 744 66. Harris, I, Osborn, T. J, Jones, P, & Lister, D. (2020) Version 4 of the cru ts monthly
745 high-resolution gridded multivariate climate dataset. *Scientific data* **7**, 1–18.
- 746 67. Gidden, M, Riahi, K, Smith, S, Fujimori, S, Luderer, G, Kriegler, E, van Vuuren,
747 D. P, van den Berg, M, Feng, L, Klein, D, et al. (2019) Global emissions pathways
748 under different socioeconomic scenarios for use in CMIP6: a dataset of harmonized
749 emissions trajectories through the end of the century. *Geoscientific Model Develop-*
750 *ment Discussions* **12**, 1443–1475.
- 751 68. O’Neill, B. C, Tebaldi, C, Van Vuuren, D. P, Eyring, V, Friedlingstein, P, Hurtt, G,
752 Knutti, R, Kriegler, E, Lamarque, J.-F, Lowe, J, et al. (2016) The Scenario Model In-
753 tercomparison Project (ScenarioMIP) for CMIP6. *Geoscientific Model Development*
754 **9**, 3461–3482.
- 755 69. Van Vuuren, D. P, Kriegler, E, O’Neill, B. C, Ebi, K. L, Riahi, K, Carter, T. R,
756 Edmonds, J, Hallegatte, S, Kram, T, Mathur, R, et al. (2014) A new scenario frame-
757 work for climate change research: scenario matrix architecture. *Climatic Change*
758 **122**, 373–386.
- 759 70. Kriegler, E, Bauer, N, Popp, A, Humpenöder, F, Leimbach, M, Strefler, J, Baum-
760 stark, L, Bodirsky, B. L, Hilaire, J, Klein, D, et al. (2017) Fossil-fueled development
761 (SSP5): an energy and resource intensive scenario for the 21st century. *Global Envi-*
762 *ronmental Change* **42**, 297–315.

- 763 71. Fricko, O, Havlik, P, Rogelj, J, Klimont, Z, Gusti, M, Johnson, N, Kolp, P, Strubeg-
764 ger, M, Valin, H, Amann, M, et al. (2017) The marker quantification of the Shared
765 Socioeconomic Pathway 2: A middle-of-the-road scenario for the 21st century. *Global*
766 *Environmental Change* **42**, 251–267.
- 767 72. Cannon, A. J, Sobie, S. R, & Murdock, T. Q. (2015) Bias correction of GCM pre-
768 cipitation by quantile mapping: How well do methods preserve changes in quantiles
769 and extremes? *Journal of Climate* **28**, 6938–6959.
- 770 73. Cayan, D. R, Maurer, E. P, Dettinger, M. D, Tyree, M, & Hayhoe, K. (2008) Climate
771 change scenarios for the California region. *Climatic Change* **87**, 21–42.
- 772 74. Artzy-Randrup, Y, Alonso, D, & Pascual, M. (2010) Transmission intensity and drug
773 resistance in malaria population dynamics: implications for climate change. *PloS one*
774 **5**, e13588.
- 775 75. Laneri, K, Paul, R. E, Tall, A, Faye, J, Diene-Sarr, F, Sokhna, C, Trape, J.-F, &
776 Rodó, X. (2015) Dynamical malaria models reveal how immunity buffers effect of
777 climate variability. *Proceedings of the National Academy of Sciences* **112**, 8786–8791.
- 778 76. Cervellati, M, Esposito, E, & Sunde, U. (2022) Epidemic shocks and civil violence:
779 Evidence from malaria outbreaks in africa. *The Review of Economics and Statistics*
780 **104**, 780–796.
- 781 77. Hsiang, S. (2016) Climate econometrics. *Annual Review of Resource Economics* **8**,
782 43–75.
- 783 78. Schlenker, W & Roberts, M. J. (2009) Nonlinear temperature effects indicate severe
784 damages to us crop yields under climate change. *Proceedings of the National Academy*
785 *of sciences* **106**, 15594–15598.
- 786 79. Hsiang, S. M, Meng, K. C, & Cane, M. A. (2011) Civil conflicts are associated with
787 the global climate. *Nature* **476**, 438–441.
- 788 80. Deschênes, O & Greenstone, M. (2007) The economic impacts of climate change:
789 evidence from agricultural output and random fluctuations in weather. *American*
790 *economic review* **97**, 354–385.
- 791 81. Kipruto, E. K, Ochieng, A. O, Anyona, D. N, Mbalanya, M, Mutua, E. N, Onguru,
792 D, Nyamongo, I. K, & Estambale, B. (2017) Effect of climatic variability on malaria
793 trends in baringo county, kenya. *Malaria journal* **16**, 1–11.
- 794 82. Moran, A. E, Oliver, J. T, Mirzaie, M, Forouzanfar, M. H, Chilov, M, Anderson, L,
795 Morrison, J. L, Khan, A, Zhang, N, Haynes, N, et al. (2012) Assessing the global
796 burden of ischemic heart disease: part 1: methods for a systematic review of the
797 global epidemiology of ischemic heart disease in 1990 and 2010. *Global Heart* **7**,
798 315–329.

- 799 83. Mabaso, M. L, Craig, M, Ross, A, & Smith, T. (2007) Environmental predictors
800 of the seasonality of malaria transmission in africa: the challenge. *The American*
801 *journal of tropical medicine and hygiene* **76**, 33–38.
- 802 84. Bhatt, S, Weiss, D, Cameron, E, Bisanzio, D, Mappin, B, Dalrymple, U, Battle,
803 K, Moyes, C, Henry, A, Eckhoff, P, et al. (2015) The effect of malaria control on
804 *Plasmodium falciparum* in Africa between 2000 and 2015. *Nature* **526**, 207–211.
- 805 85. Li, C & Managi, S. (2022) Global malaria infection risk from climate change. *Envi-*
806 *ronmental Research* **214**, 114028.